DOI: 10.1002/anie.201201114

Multivalency

Multivalency as a Chemical Organization and Action Principle

*Carlo Fasting, Christoph A. Schalley, Marcus Weber, Oliver Seitz, Stefan Hecht, Beate Koksch, Jens Dernedde, Christina Graf, Ernst-Walter Knapp, and Rainer Haag**

Keywords:
cell recognition · cooperative phenomena · multivalency · receptors · supramolecular chemistry

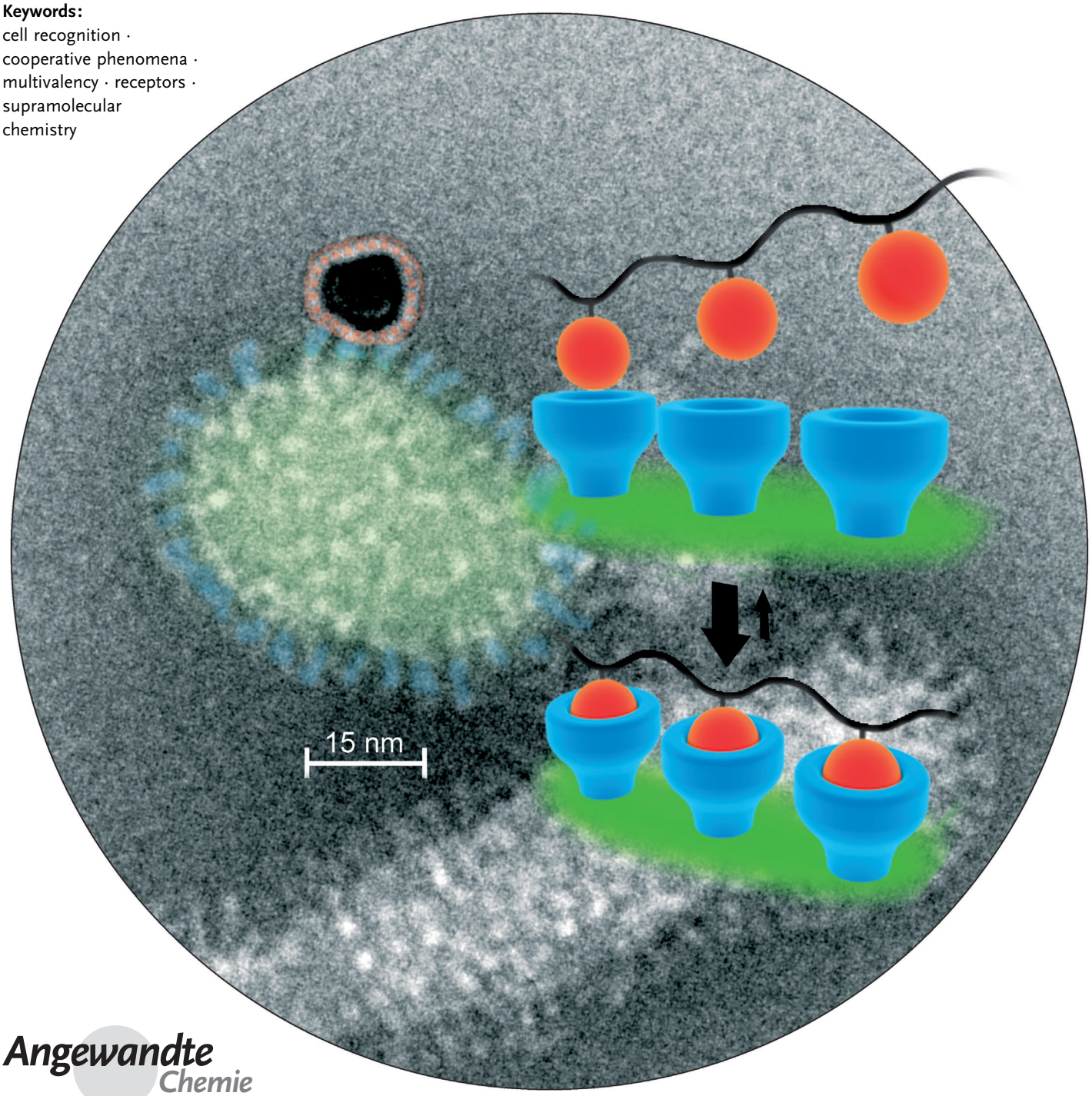

Multivalent interactions can be applied universally for a targeted strengthening of an interaction between different interfaces or molecules. The binding partners form cooperative, multiple receptor–ligand interactions that are based on individually weak, noncovalent bonds and are thus generally reversible. Hence, multi- and polyvalent interactions play a decisive role in biological systems for recognition, adhesion, and signal processes. The scientific and practical realization of this principle will be demonstrated by the development of simple artificial and theoretical models, from natural systems to functional, application-oriented systems. In a systematic review of scaffold architectures, the underlying effects and control options will be demonstrated, and suggestions will be given for designing effective multivalent binding systems, as well as for polyvalent therapeutics.

From the Contents

1. Introduction

Multivalency is a key principle in nature for achieving strong, yet reversible interactions. The burr and its man-made analogous material, velcro, are good examples from daily life (Figure 1). By allowing multiple hooks on one side to entangle with loops on the other, a large number of weak interactions can strongly connect the two surfaces and, for example, protect against shearing. The greater the fleece surface, the stronger the binding. Reversibility by sequentially separating the individual hooks and loops is, therefore, an important way to differentiate between multivalent and covalent reactions. The latter case would represent, technically speaking, a permanent adhesive or a series of screws.

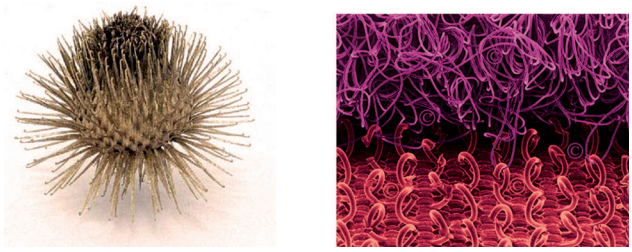

Figure 1. The principle behind the burr (left) and nature-inspired velcro (right) can be transposed to the molecular level.

On the molecular level, one can compare the hooks seen in the macroscopic example from nature with specialized molecular binding units (ligands) and the corresponding loops with the binding pockets in a complex molecule (receptor). Biologically speaking, such multivalent interactions between cells or with other organisms, such as bacteria and viruses, are medically very important, wherein the extensive interaction between a large number of individual, mutually binding partners plays a major role.

In contrast to weak monovalent binding, multivalent interactions offer the advantage of a multiple and thus dramatically enhanced binding on a molecular scale. An important example is the multivalent interaction between a virus and its host cells that initially leads to a stable adhesion (Figure 2a). The virus can subsequently be engulfed by the cell membrane and taken up through a process called endocytosis. Insertion of the viral genome into the cellular DNA ultimately results in the formation of new virus particles. The current therapeutic approach in medicine is to employ monovalent drugs. Since the virus has a high affinity for the multivalent binding sites of the cell surface, monovalent drugs can only be effective in very high doses

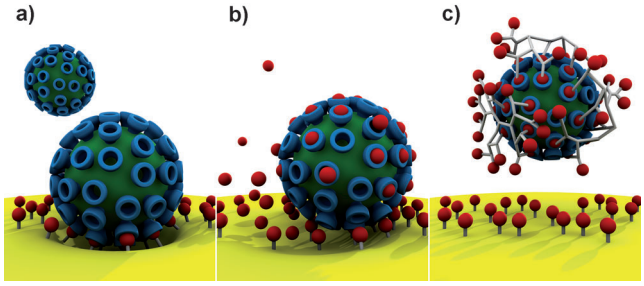

Figure 2. a) A multivalent binding of a virus to a cell surface is compared to b) a noncompetitive binding with monovalent ligands (classical drug approach). c) Multi- and polyvalent ligands are considerably more effective in binding and shielding a virus surface than monovalent ligands, thus preventing viral adhesion.

[*] Dr. C. Fasting, Prof. C. A. Schalley, Prof. B. Koksch, Prof. C. Graf, Prof. E.-W. Knapp, Prof. R. Haag
Institut für Chemie und Biochemie
Freie Universität Berlin
Takustrasse 3, 14195 Berlin (Germany)
E-mail: haag@chemie.fu-berlin.de

Dr. M. Weber
Konrad-Zuse-Zentrum für Informationstechnik Berlin (Germany)

Prof. O. Seitz, Prof. S. Hecht
Institut für Chemie der Humboldt-Universität zu Berlin (Germany)

Dr. J. Dernedde
Zentralinstitut für Laboratoriumsmedizin
Klinische Chemie und Pathobiochemie
Charité-Universitätsmedizin Berlin (Germany)

(Figure 2b). As a result, the synthesis and investigation of multivalent scaffold architectures have enormous potential for competitively and effectively fighting viruses and bacteria (Figure 2c).

In addition to the stronger bonds resulting from multivalency that let the cell membrane successfully take up a virus once it has adhered itself, another important feature is that one can control shape in multivalent reactions, even on a large scale. Since the arrangement of the binding sites on multivalent ligands can influence the geometry of the receptors on the membrane of the host cell, they can introduce predefined large-scale functional architectures that are especially suitable for clustering and cellular uptake.

In this Review, multivalency is defined in terms of multiple, interconnected supramolecular binding modules in both biological as well as synthetic systems. So far, however, the studies on multivalent reactions in synthetic systems have not been as varied and significant as in biological systems. Although there have only been a few explicit and systematic investigations of host–guest systems for application in a multivalent construct, some important insights could still be obtained. One major advantage of synthetic systems is that a set number of defined binding sites can be chemically controlled, with the result that a quantitative thermochemical analysis may be performed. Furthermore, synthetic structures are often varied systematically with a reasonable amount of effort so that a series of host–guest complexes may be examined in detail. Thus, not only monovalent and multivalent but also intermediate interaction scenarios can be investigated. Furthermore, the spacers, which connect the binding sites to one another, are variable. Consequently, they are not just "innocent observers", because they strengthen or weaken the ligand binding by interacting with the receptor or its neighboring binding sites.

The targeted use of multivalency is, therefore, of great importance not only for medicine,[1,2] (e.g. for the production of anti-infectives) and biochemistry,[3] but also for the design of new structurally defined functional molecules in supramolecular chemistry[4,5] and materials science.[6] Multivalent molecular systems can be used to build a controlled self-assembly of increasingly complex structures or to achieve a targeted chemical nanostructuring of surfaces.[7]

Earlier reviews on multivalent binding[1,3–5,8–10] will not be repeated here. Instead, the goal will be to develop a fundamental understanding of multivalency as a chemical organization and action principle and to present critical factors that will afford the most efficient multivalent interactions. Selected examples of multi- and polyvalent interactions as well as their potential applications will provide further insight into the current state of research and illustrate the theoretical principles of multivalency. The focus of this Review will be to compare synthetic multi- and polyvalent scaffold architectures, which are responsible for the presentation of ligands.

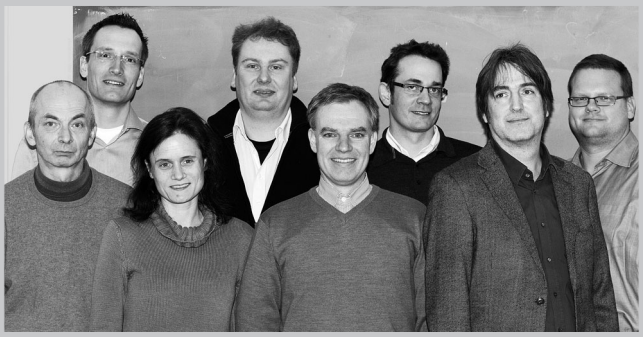

From left to right: J. Dernedde, S. Hecht, C. Graf, M. Weber, R. Haag, C. Fasting, O. Seitz, C. A. Schalley (missing from picture: B. Koksch and E.-W. Knapp). The author team is part of the collaborative research center (SFB) 765 "Multivalency as Chemical Organization and Action Principle: New Architectures, Functions and Applications", which has been funded by the German Research Foundation since 2008 and consists of around 80 scientists in 21 scientific research projects at various research institutions in Berlin (speaker: Rainer Haag, FU Berlin) and includes an integrated graduate school that currently has 35 graduate students. For more information see: www.sfb765.de.

2. Multivalent Interactions

2.1. Terms and Definitions

Interactions between an m-valent receptor and an n-valent ligand ($m,n>1$; also $m\neq n$) are considered to be multivalent. Interactions between a number of monovalent ligands ($n=1$) with a multivalent receptor are not multivalent. However, the number m of equivalent binding pockets in a multivalent receptor already gives monovalent ligands favorable conditions for interaction, because an m-valent receptor binds to the monomeric ligand m times more often than a corresponding monovalent receptor. This symmetry effect[11–13] is induced by the equivalent binding pockets of the m-valent receptors and correspondingly also occurs with multivalent ligands. If the receptor or ligand has multiple identical binding sites, they are homomultivalent. If they have multiple binding sites, which are different from each other, they are considered to be heteromultivalent.

The term polyvalency often appears in the literature, especially in the context of ligands binding to receptors on interfaces such as cell membranes, which offer a large number ($n\gg10$) of two-dimensionally distributed binding sites.[2] In this Review, multivalency and polyvalency are not differentiated in the conventional sense, because the large number of binding sites on the interface necessitates that symmetry factors[11] are taken into account for a precise description. This problem not only occurs, for example, on interfaces, but also if a decavalent receptor reacts in solution with a divalent ligand. Therefore, a description of both phenomena must be treated in the same way. However, a linguistic distinction between multi- and polyvalence might be useful to differentiate between studies on isolated multiple interactions and the usually highly dynamic and, therefore, less-defined interfacial interactions.

Avidity is a concept that comes from biochemistry and was originally introduced to describe the binding behavior of immunoglobulins with different valencies (antibodies, IgD, IgEm, and IgG monomers: divalent; IgA homodimer: tetravalent; IgM homopentamer: decavalent). Hence, the concept of avidity in terms of antibody binding is comparable

to multivalency, but will not be treated here in depth (see Ref. [1]). Schwarzenbach's long-known chelation effect,[14] which was already introduced in 1952, is also conceptually closely related to multivalency. These two terms are sometimes used as synonyms,[4,15] with the concept of chelation traditionally appearing in inorganic coordination chemistry, and multivalency in organic and macromolecular chemistry.

Both concepts describe similar phenomena, namely, the cooperative interaction of several interconnected binding groups during a binding process. Unlike chelation, which involves a central atom or molecule, multivalency refers in general, as well as in this Review, to the interaction of multiple binding modules that are coupled to one another in biological and synthetic systems. The decisive factor here is the manner in which multiple binding modules (natural or synthetic ligands and receptors) are brought together into appropriate structures and architectures rather than by the supramolecular interactions of isolated binding modules. The above-mentioned polyvalency is more than a simple chelation effect, especially in regard to large-scale, two-dimensional interactions. Considering that nature also uses the polyvalent effect, even on a micrometer scale, one must conclude that the chelation effect, in terms of simple mononuclear metal ion/ligand complexes with their defined "multivalent" coordination spheres, is a particular example of multivalent interactions. It has also been shown[16,17] that even a "simple" chelation effect such as the binding of ethylenediaminetetraacetate (EDTA) to calcium ions can only be described with difficulty by quantitative thermodynamic analysis. This is even more so the case for complex multivalent or polyvalent biological systems.

To characterize a multivalent binding effect, Whitesides and co-workers[1] proposed an enhancement factor β, produced by taking the ratio of the binding constant for the multivalent binding [K_{multi}] of a multivalent ligand to a multivalent receptor with the binding constant for the monovalent binding [K_{mono}] of a monovalent ligand to a multivalent receptor [Eq (1)]. An advantage of this enhancement factor is that it can be used even if the multiplicity of effective binding interactions is unknown. A disadvantage is that it simultaneously also includes the influence of the cooperativity and the symmetry effect.

$$\beta = \frac{K_{multi}}{K_{mono}} \quad (1)$$

Despite repeated clarification in the literature,[4–6] there is still a widespread misconception that multivalent interactions are inherently associated with positive cooperativity.[18] A multivalency-enhanced binding may also be useful when the binding is not non-cooperative (additive) or positively cooperative (synergistic). As a result, although most multivalent systems are rather negatively cooperative (interfering), multivalent drugs can conceivably be administered in much smaller doses than the corresponding monovalent analogues without losing any more efficacy because of the stronger binding and higher specificity at the target receptor.

In all multivalent systems, the structures connecting the different ligands—as part of a rigid skeleton or even as a flexible chain—play a crucial role. In this Review, we propose to use the general term spacer regardless of the chemical nature and structure of this connecting link. We will see below that its flexibility has a significant influence on the thermodynamic description, as noticeably different symmetry factors have to be taken into consideration for very flexible and very rigid ligands.

2.2. Theoretical Background/Kinetic and Thermodynamic Aspects

The thermodynamics of the monovalent binding of a ligand to a receptor is mainly determined by the free binding enthalpy (ΔG_{mono}). Although in monovalent systems there are only two states (bound and unbound), from which the corresponding free enthalpy difference is derived, this duality is no longer present in multivalent systems. There are $n+1$ different binding states for an n-valent receptor discriminated by the number j of occupied receptors. To calculate the free binding enthalpy $\Delta G_{LR}^{(n)}$ for common multivalent systems one must first determine which binding conditions ($0<j<n$) should be considered as bound or unbound. Since the number of possibilities for j receptor sites to be occupied by an n-valent receptor is $\frac{n!}{(n-j)!j!}$ for symmetry reasons, and results in many partially occupied situations, this assignment is crucial for the expected cooperative effect of the multivalent binding.[12] Two extreme cases will be discussed. In the first, the binding effect may be measured if all the receptor sites are occupied by ligands. As a consequence of symmetry, this situation is much rarer than with partially occupied receptors if the ligands act independently of each other. A preorganization of the ligands through multivalent presentation is desirable. In the second special case, an effect already occurs if a single receptor site is occupied by just one ligand. The "first binding" is, however, entropically more difficult if the ligands are linked together. The entire entropy of a system with n receptors of n free monovalent ligands decreases only slightly when a single ligand binds to a receptor site and thus changes the solvatation, rotation, and translation entropy ($\Delta S_{mono} = \Delta S_{trans} + \Delta S_{rot} + \Delta S_{sol}$), because the still-free ligands continue to maintain the entropy. It is a different story for multivalent ligands. In this situation, several monovalent ligands are interconnected by a spacer or on interfaces. This system already loses some of its translation and rotation entropy if one individual ligand in the scaffold is connected to a single receptor site. Furthermore, the conformational entropy of the spacer architectures is reduced (ΔS_{conf}). Generally the "first binding" of a multivalent ligand to a single receptor site is, therefore, entropically hindered (see also Ref. [19]). Mammen et al.[1] show this in the following model. They assumed that the change in the entropy of the n-fold binding (excluding conformational entropy) has essentially the same contributions as the monovalent binding of a single ligand ($\Delta S_{multi} = \Delta S_{trans} + \Delta S_{rot} + \Delta S_{sol} + \Delta S_{conf}$). It is also thought that the enthalpy of the monovalent binding (ΔH_{mono}) increases in a multivalent binding regardless of the spacer ($\Delta S_{multi} = n\Delta H_{mono}$), so that the difference in the free binding enthalpies

is $\Delta\Delta G = \Delta G_{LR}^{(n)} - n\Delta G_{mono} = T(n-1)\,\Delta S_{mono} - T\Delta S_{conf}$. Two conclusions may be drawn from this equation: 1) There will be a large loss of conformation entropy with flexible spacers. The cooperative effect is also not expected to be as strong as with a rigid spacer. 2) A small number of binding valences is less efficient because of entropy. High valences are preferable. A special case is when the multivalent ligand architecture only allows binding states with $j=0$ and $j=n$. This behavior fits best to rigid, tailor-made chelate compounds which bind to metals with multiple binding sites.[20,21]

In the above model by Mammen et al., the spacer was not presumed to provide any enthalpic contribution to the binding. In fact, the assumption that $\Delta H_{multi} = n\Delta H_{mono}$ may be very unrealistic. First of all, the spacer could positively or negatively interact with the receptor because of its chemical nature and thus change the multivalent binding enthalpy. Secondly, an inexact geometric preorganization of the ligands could cause an enthalpic weakening of the multivalent binding. Thirdly, a spacer may directly affect the (e.g. electrostatic) characteristics of the ligands and lead to a change in the binding affinity. These effects can be easily studied with theoretical methods, such as molecule dynamics, and are very helpful because the systematic exchange of spacer groups usually requires elaborate synthetic operations. A combination of entropic and enthalpic effects is possible if the preorganization of the spacer is imperfect, but allows the ligands to be optimally geometrically oriented because of the flexibility of the spacers (Figure 3).

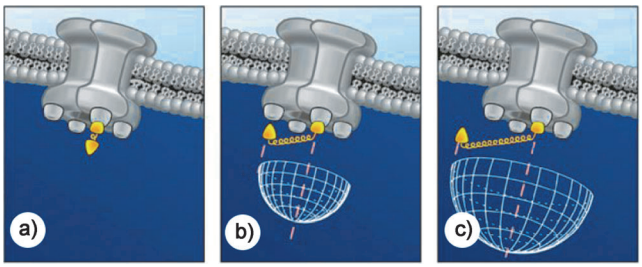

Figure 3. Divalent binding of a ligand to the tetravalent cGMP receptor. a) If the spacer is too short, only one binding site may be occupied in the receptor. b) The highest binding affinity is achieved with an adequate spacer length and optimal operating range for the second binding. c) Too long a spacer again increases the number of unproductive degrees of freedom and reduces the binding affinity. Figure from Ref. [24] by courtesy of Macmillan Publishers Ltd.

In this simple model it is assumed that the entropy and enthalpy contributions of the solvent during a multivalent reaction can be derived from the monovalent binding case. However, the existence of a spacer could introduce in some cases a number of weak interactions into the system that might cause an entropy–enthalpy compensation during the binding process because of greater differences in heat capacity. Solvent effects should, therefore, be taken into account in molecular simulations with explicit modeling (see Section 2.4). Furthermore, one should not disregard that an additional spacer structure may have an influence on the entropic and enthalpic properties of the interacting ligand and receptor moieties.[22,23]

From a thermodynamic standpoint, the multivalent presentation of ligands is not always advantageous. For a more detailed analysis of the multivalent binding between a ligand and a receptor it is important to determine not only their geometries but also the nature and number of system states made possible by flexibility.[221] It is also necessary to define whether a state is "bound" or "unbound."

This definition is not only based on the number of occupied receptor sites, but also on the spatial proximity of the multivalent ligand to the receptor. In this case, it does not matter how many interactions exist between the two partners. Proximity is essential if the ligands are to actively intervene in the binding process. Once a single ligand of a multivalent system is attached, the probability that other neighboring ligands will also bind becomes higher. An experiment by Kramer and Karpen[24] demonstrated that this effect can be measured. Models that were already conceptualized in 1925 by Kuhn[25,26] and later applied for multivalency[27] are based on a highly effective local concentration of ligands, if the first ligand is bound to the receptor. A closer look, however, has shown that the position of the second ligand (in a divalent system) stays relative to the first in a three-dimensional Gaussian distribution[19] and thus does not spread homogeneously. As a result, the increased local concentration is often significantly overestimated.

It is a common practice, however, to evaluate the first binding event between multivalent ligands and receptors differently in terms of kinetics, because the first binding process produces the spatial proximity that leads to a higher local concentration. While the first binding process may be kinetically seen as an intermolecular process that is determined by the receptor and ligand concentration, the second and all subsequent binding processes can be viewed as intramolecular processes which will then only be determined by the ligand concentration. The total equilibrium constant of a divalent binding process, thus, contains a factor that has the unit of a concentration and is called "effective molarity" (EM). It can be measured for divalent systems (see Section 2.3). As a result of the above-described thermodynamic aspects, the "first binding" of a multivalent system usually has a lower binding rate than a monovalent system. The following binding events are faster because of the preorganization of the ligands. The binding kinetics of a multivalent system is, therefore, an ensemble quantity and can be regarded as a weighted average for many different elementary binding processes. The proximity of a ligand to its receptor, therefore, significantly determines the probability of the corresponding binding process.

In their work on divalent binding behavior, Mack et al. were able to study the proximity of a soluble, divalent receptor to the ligand surface by defining "unbound" and "preoriented" states,[28] wherein receptor–ligand interactions are only successfully formed from such preoriented states. A ligand may have converged from solution to the interface or have partially or completely dissociated from the receptor surface before the binding event occurs. In the latter case, it is highly probable that spatial proximity allowed them to reconnect (rebinding). By using His-tags of different lengths, Ernst and co-workers demonstrated that an effective rebind-

ing may be measured in terms of a multivalent ligand "sliding" onto a (multivalent) surface rather than a complete dissociation in a flow system such as surface plasmon resonance (SPR).[29]

Recent mathematical research on protein folding has indicated that mixing spatial and kinetic aspects in a kinetic approach is limited. It is not possible theoretically to arbitrarily predefine all the elementary steps of an entire system, as it may lack the corresponding individual kinetic entities. No rate constants could be measured for these spatially predefined states.[30] The predefinition of individual elementary processes results in an incomplete and incorrect description of the reality. From a mathematical point of view, an arbitrary decomposition of the continuous kinetic process, especially into only a few fundamental steps, destroys the so-called Markov property,[31–33] which basically means that the system does not have a memory. To correctly formulate the kinetics, it is necessary to choose system-dependent elementary steps, which leads to the scenario that some binding states can no longer be clearly classified as "bound" or "unbound".[34,35] Therefore, other factors such as ligand and receptor structure, diffusion, and laminar transfer (at interfaces) also have to be taken into account in a mathematical kinetic analysis of multivalent interactions.

2.3. Multivalency and Cooperativity: Determining Effective Molarities

In biological systems, the number of binding sites is often not known, which makes it impossible to come to a conclusion on the cooperativity of a multivalent binding. However, this is not the case for synthetic materials, as the number n of binding sites can be directly adjusted during synthesis or can be determined in a final stage by using common analytical methods. As a result, individual contributions to the multivalent binding may be determined and statements on the cooperativity can be made;[36,37] the determination of the effective molarity EM plays a particularly crucial role. A divalent example is shown in Figure 4, whereby EM is the critical concentration under which ring closure to a divalent complex and not oligimerization is the preferred result.

If we consider the final equilibrium between the open and closed form of the divalent complex, the term $K_{mono}EM$ is an expression of cooperativity. If $K_{mono}EM$ is $\gg 1$, the divalent binding shows positive cooperativity. If there is negative cooperativity ($K_{mono}EM \ll 1$), the divalent complex is mostly present in the open form.[36]

The effective molarity can be determined by "double mutant cycles", as shown in Figure 5 for a divalent pseudorotaxane,[38] and elegantly applied by Hunter and co-workers in a number of experiments.[39–41] It is

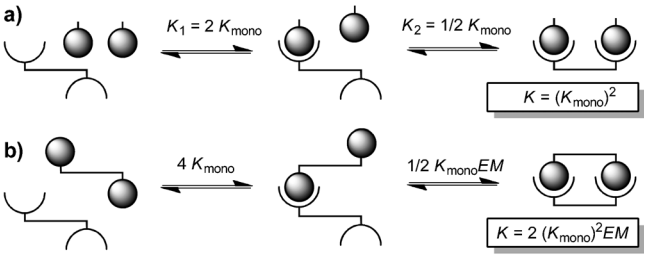

Figure 4. Binding constants of individual equilibria (K_1 and K_2) and the total binding constants ($K = K_1 \cdot K_2$) for the successive binding of a) monovalent and b) divalent guests by a divalent host.

necessary to look at the disproportionation equilibrium from which first the equilibrium constants and then the EM can be easily obtained from the constants K^A–K^D, which are independently measureable [Eq. (2)]. The larger the EM, the more the equilibrium is located on the side of the divalent complex and the more strongly the reaction is positively cooperative.

$$K = \frac{K^A K^D}{K^B K^C} = \frac{2K^2_{mono} EM K^2_{mono}}{K^2_{mono} K^2_{mono}} = 2EM \qquad (2)$$

An interesting observation is that the pseudorotaxane with the $O(CH_2)_2O$ spacer in the center of the axis clearly shows a positive cooperativity ($EM = 132$ mM; $K_{mono}EM \approx 40$). However, insertion of only a single additional methylene group results in an almost noncooperative binding ($EM = 5.8$ mM; $K_{mono}EM \approx 2.5$). This effect can be explained by an attractive stacking interaction between the anthracene

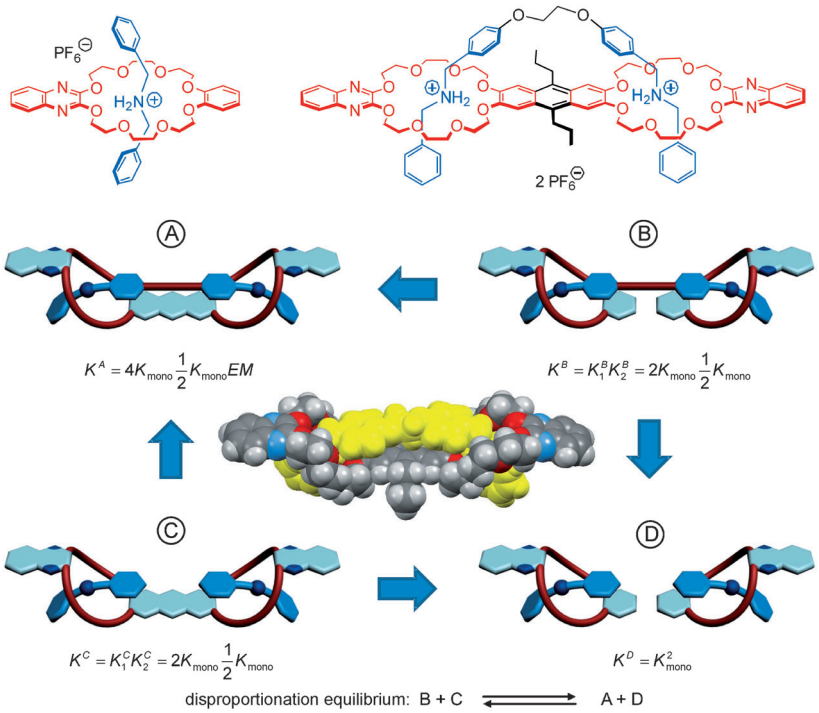

Figure 5. Determining the effective molarity for formation of a divalent pseudorotaxane by a double mutant cycle. The crystal structure of the pseudorotaxane is shown in the middle (dark gray C, light gray H, red O, blue N, yellow bivalent ligand).

spacer in the crown ether dimer and the two inner phenyl groups in the axis. The crystal structure (Figure 5, middle) shows that the $O(CH_2)_2O$ spacer is ideally suited for this purpose, while longer spacers will interfere with its geometry.

The divalent pseudorotaxanes have rather flexible spacers in their axes and are characterized by only a small cooperativity. In contrast, the *EM* values for binding the hexapyridine guest in the hexavalent porphyrin wheel shown in Figure 6 are higher by one order of magnitude ($EM = 280$–1700).[42,43] Such highly effective molarities and distinctly positive cooperativity for this supramolecular interaction can be attributed to an almost perfect preorganization and to the high rigidity of both the host and guest.

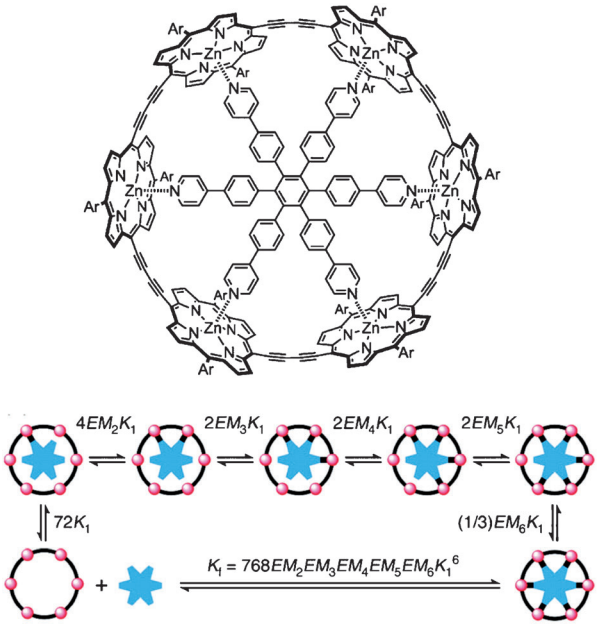

Figure 6. Extreme chelate cooperativity can be found in this perfectly preorganized, hexavalent complex from Anderson's porphyrin wheel. Figure from Ref. [42] by courtesy of the American Chemical Society.

The various individual interactions between the host and guest at the interacting binding groups can be broken down into individual contributions, again with the help of "double mutant cycles". Hunter et al. were able to do this, for example, with zinc porphyrin, to which guests were not only bound by coordination of the pyridine nitrogen atom to the central Zn^{II} ion: In these host–guest complexes, hydrogen bonds in the complex periphery also linked the host–guest system together and their individual contributions could be accurately determined.[44] These systems were recently quantified for neighboring effects,[45] and the effective molarities for the formation of hydrogen bonds proved to be significantly solvent-dependent.

2.4. Modeling/Calculations of Multivalent Interactions

The conformational entropy of the binding unit between the individual receptors or ligands plays an important role in the investigation of multivalent interactions. Simplified theoretical models depict the spacer as a chain of abstract elements that can only be arranged in a set way to each other.[46–50] These simplified models are often not accurate enough for estimating the conformational entropy of a spacer. They disregard the physical interactions of the atoms with one another in the spacer or with the solvent. In particular, the behavior of a spacer also depends on the type of ligand to which it is bound. There is, therefore, a need for a physical model of the system comprising the solvent, spacer, and ligand that will take into account these interactions. For example, an accurate atomistic, chemical physical model of the system can be provided by molecular-modeling studies.[51] The behavior of the spacer–ligand–solvent system can be computationally simulated and the entropic properties of the spacer evaluated with the help of statistical thermodynamics.

There are many different approaches that can be used to determine the conformational entropy from statistical data. One approach is to consider entropy as temperature-dependent on the free energy.[52,53] In this case, simulation data are generated at different (theoretical) temperatures, which is associated with much computational effort. Alternatively, one may use the relationship between the variance of random samples and the entropy (assuming a normal distribution of degrees of freedom). The assumption that there is a normal distribution for the investigated degree of freedom may be inaccurate and must be corrected if necessary. Another approach is to prepare entropy estimations directly from the simulation data.[54] In this approach, it is possible to consider the solvent on the atomic level (explicit) rather than with models, where only location-independent physical properties of the solvent can be introduced (implicit).

It has been shown in an explicit approach[55] that the influence of ligands on the entropic properties of the ligand–spacer–solvent system cannot be neglected, as is the case with simplified models. For example, if two ligands with hydrophobic properties (such as the estrogen receptor agonist diethylstilbestrol, DES) are connected through a flexible spacer (e.g., based on polyethylene glycol, PEG), hydrophobic interactions between the ligands reduce the conformational entropy of the spacer in the water solvent (compared to the pure PEG spacer). This restricts the freedom of the ligands so much that the above-described negative cooperative effect prevails and a divalent system is no longer more advantageous in terms of free energy than using two monovalent binding ligands. Such preceding ligand–ligand interactions can only be suppressed by rigid spacers (Figure 7, see also Section 3.2.2).

In addition to determination of the conformational entropy of the spacer, an accurate atomistic simulation of multivalent binding processes is also a challenge for computer-aided methods. Currently, theoretical groups are primarily working on differences in the free energy between the monovalently bound and the unbound ligands (binding affinity), but many of the methods used fail in the multivalent binding process.[56] To determine the difference in free energy of a monovalent binding process by molecular modeling, two scenarios will be simulated and finally compared: first, a fully solvated ligand molecule and secondly, the ligand in its

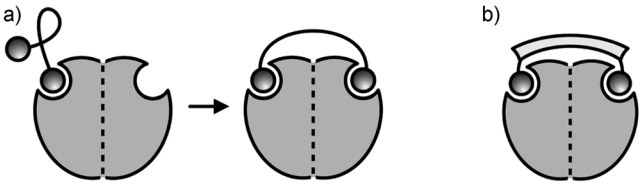

Figure 7. Several methods for divalent binding, in which the spacer substantially participates. a) A flexible spacer avoids linear conformation by entropically preferential folding and aggregation. A linear conformation is only accepted due to binding of a second ligand. b) A rigid spacer with flexible short end groups immediately avoids entropic losses arising from reduced degrees of freedom and preorientation of the ligands.

"binding position" within the binding pocket of the receptor. This type of modeling presumes the binding process to be a single-stage transition between the "bound" and "non-bound" state. The difference in free energy $\Delta\Delta G$ of these two end points also determines the ratio of the reaction rates r_{12}, r_{21} of a reversible association: $\Delta\Delta G = -k_B T \ln\left(\frac{r_{12}}{r_{21}}\right)$. This Equation does not work for a multivalent binding process because there are always different states ("does not bind a ligand", "binds one", "binds two" …), which have an impact on the equilibrum. The simulation of individual scenarios will, therefore, not lead to further insights into the process rates.[35] In fact, it is the free energy barriers that provide information about the process rates. Conformational dynamics is a method that focuses on the study of the energy barrier of molecular processes.[57,58] It has already been shown this way that even a monovalent binding process can proceed in several stages.[59] However, there have been very few investigations on multivalent binding processes by means of such theoretical methods.[221]

2.5. Quantification of Multivalent Interactions

Several techniques have already been used to quantify multivalent interactions. Association and dissociation constants can be determined, for example, by fluorescence spectroscopy,[60] total internal reflection fluorescence spectroscopy and microscopy (TIRFS, TIRFM),[61,62] or by quartz crystal microbalance (QCM) measurements.[63] Thermodynamic and kinetic parameters are available for the quantification of multivalent interactions by surface plasmon resonance (SPR) spectroscopy,[64] isothermal titration calorimetry (ITC),[65] and for binding constants $< 10^5$ by NMR spectroscopy. Atomic force microscopy (AFM) and related methods allow a direct measurement of binding strength.[66] It is possible to determine the colloidal stability of nanoparticle systems depending on their multivalent stabilization by using microscopy and dynamic light scattering methods, as well as to measure multivalent interactions of induced aggregation.[60,67] Various biological assays are used to evaluate multivalent interactions in biological systems. The label-free SPR detection method is most commonly used. SPR enables the determination of binding constants, when there is a 1:1 binding mode of a receptor–ligand couple.

Although this method may also be applied to low-valent ligand conjugates,[68] experimental data, especially for high-valent ligand conjugates with a complex architecture, can often not be assigned a binding model and thus not fully evaluated. An alternative to describe multivalent interactions is offered by the determination of IC_{50} values by using SPR. This value is defined as the ligand concentration which corresponds to a reduction of the binding signal to 50% of the initial value. Thus, the smaller the IC_{50} value is, the more potent the inhibitor. As soon as a robust SPR assay for the receptor–ligand interaction has been established, the concentration-dependent inhibition of the receptor with potential multivalent inhibitors can be easily determined. Standardization of a functionality or a ligand allows one to determine the enhancement factor β, which describes the average affinity of a multivalent ligand system.

Some advantages of this competitive binding approach are that a large number of samples may be analyzed with high reproducibility and relatively quickly compared, and that only a few samples are required because of its high sensitivity, , which is important in for many biological studies. This measuring method can also be used to compare interactions that take place in vivo under flow conditions, such as bacterial and leukocyte adhesion in blood vessels (see Section 4.2).

Table 1 shows some of the most important techniques for quantifying multivalent interactions in terms of the measurement techniques and physicochemical parameters including some specific examples.

3. Multivalent Scaffold Architectures

To use multivalency as a principle for organization and action, it is necessary to intelligently design a structure of multivalent ligands that not only takes into account the intrinsic affinity of each ligand but also their distance and relative spatial orientation (preorganization). These issues are largely determined by the choice of scaffold and the architecture of the spacer, which can be achieved in two extremely different ways. The first is a flexible linkage of individual ligand units, which allows the system a great deal of conformational space, but only a small fraction of them present "productive" structures in terms of a multivalent interaction. In regard to statistical thermodynamics, multivalent binding processes lead to a loss in conformational entropy in the backbone (see Section 2.2). In the second approach, this loss of entropy is hindered by rigidly attaching the ligand units, but this requires the ligands to be optimally oriented to avoid a large loss of binding enthalpy. Since such precision can be achieved in only a few cases, the most promising path to take appears to be, as usual, a middle road that allows just enough flexibility for attachment and nothing more.

An additional and often critical component in the course of this binding process are changes in the solvation of the backbone. Thus, the spacer may be solvated to different degrees as a result of changing conformations and therefore be subjected to unspecific interactions such as hydrophobic adsorption to the receptor surface. The overall solvation

Table 1: Measurement methods for quantifying multivalent interactions.

Technique	Measurement parameters	Measure of multivalency	Examples
UV/Vis/NIR absorption spectroscopy	transition temperature (from the change in absorption) as a function of host concentration	binding enthalpy	hybridization of oligothymine templates (host) with oligomeric adenine and naphthalene diaminotriazine guests[69]
	apparent deflection temperature (from the change in absorption) as a function of guest concentration	guest–guest interaction energy	
	change in absorption as a function of ligand concentration	association constant	
fluorescence spectroscopy	relative change in fluorescence intensity as a function of ligand concentration	association constant	multivalent interaction of carbohydrate-modified quantum dots with lectins and sperm[60]
	complexation degree of the host molecules (determined from fluorescence intensity) as a function of the concentration of guest molecules	association constant	host–guest interaction between the periphery of adamantyl-urea-functionalized dendrimers and ureido-acetic acid derivatves[70]]
total internal reflection fluorescence (TIRF) microscopy/spectroscopy	fluorescence intensity as a function of the concentration of the multivalent protein ligand	association constant	two-dimensional protein–protein interactions on model membranes[61]
		dissociation constant	interaction of multivalent protein ligands with lipid bilayers[62]
		dissociation constant	interaction of cholera toxin and phospholipid membranes[83]
surface plasmon resonance (SPR) spectroscopy	refractive index changes in ligand-receptor interaction (mass-dependent)	association constant, IC_{50}	affinity screening of antibodies[71] multivalent interactions between selectins and polyglycerol sulfates[72]
circular dichroism (CD) spectroscopy	CD intensity as a function of the host/guest concentration	guest–guest interaction energy	hybridization of oligothymine templates with oligomeric adenine and naphthalene diaminotriazine guests[69]
NMR spectroscopy	diffusion coefficients from DOSY measurements[73]	size information for detecting multivalent-induced complex formation	hexameric resorcinarene and pyrogallarene capsules[75]
	NMR signal integrals or shifts as a function of the ligand–receptor ratio and NMR titration[74]	free binding energy temperature-dependent measurements: binding enthalpy and entropy activation parameters ΔG^{+}, ΔH^{+}, ΔS^{+}, for example, by lineshape analysis	
EPR spectroscopy	dipolar interaction between spin probes	distance distribution in solution structural changes	measurement of the distance between divalent spin probes in solution[76]
isothermal titration calorimetry (ITC)[65]	heat as a function of the ligand/receptor or host/guest ratio	association constant binding enthalpy binding entropy free binding enthalpy	maltose and lactose on the surface of β-cyclodextrin vesicles[77] threading of pseudorotaxanes[78]
laser reflection interferometry (LRI, Rif)	reflectivity or resultant coverage degree with bound ligands as a function of time	dissociation and association constants	two-dimensional protein–protein interactions on model membranes[57]

Table 1: (Continued)

Technique	Measurement parameters	Measure of multivalency	Examples
quartz crystal microbalance (QCM)	frequency change as a function of the multivalent ligand concentration	association constant	multivalent interaction of lectins with a cross-linked, surface-grafted glycopolymer[63]
atomic force microscopy (AFM)	pulling force as a function of the intermolecular distance	binding strength	molecular interaction between bacteriophages and lipopolysaccharide bilayers[66] intermolecular interactions between C_{60} and porphyrin derivatives[79]
transmission electron microscopy (TEM)	number of (multivalent) nanoparticles per aggregate	degree of aggregation induced by multivalent functionalization	multivalent carbohydrate-modified quantum dots interact with lectins and sperm[60]
	visualization of individual bindings in a multivalent complex	stability against aggregation as a function of multivalent functionalization	binding of virus particles to nanoparticles[80,81]
fluorescence microscopy	fluorescence intensity as a function of time	rate constant	binding of CdS quantum dots with variable ligand multivalency of GABA(C) receptors on a cell membrane[82]
dynamic light scattering (DLS)	hydrodynamic diameter (from temporal change of the scattering intensity) as a function of time	aggregation rate constant (to measure stability versus aggregation through multivalent stabilizing	aggregation of mono- and multivalently thiol-stabilized gold nanoparticles in solution[67]
high-performance liquid chromatography (HPLC)	difference in retention as a function of polarity and molecular size	competitive measurements enable determination of equilibrium constants	trivalent interaction between vancomycin trimer and D-Ala-D-Ala trimer[84]

contributions of ligand binding should be nearly identical in monovalent and multivalent interactions. As these complex relationships substantially complicate an experimental investigation of the phenomena, mostly only isolated observations or reports of successful multivalent ligand conformations appear in the literature. There are still too few systematic and comparative studies on the influence of the scaffold architecture on the strength of multivalent interactions. The following section will focus on and discuss several exemplary structure types and their advantages and disadvantages.

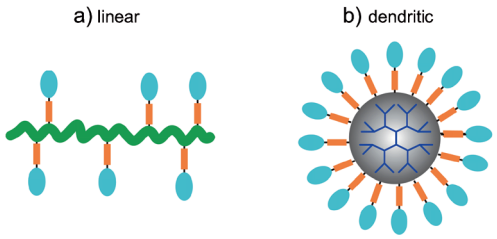

Figure 8. Examples of synthetic polymers which are used as scaffold architectures for multivalent interactions (light blue: ligand, orange: spacer).

3.1. Statistical Polyvalence

3.1.1. Synthetic Polymers

Great flexibility and adjustable solubility make multifunctional organic polymers an appropriate platform for anchoring ligands to enable polyvalent interactions (Figure 8). Linear structures were first used for statistic multivalence and have been applied, for example, to inactivate viruses (see Section 4.2) by specific interactions between sialic acid (SA) functionalized polyacrylamides and hemagglutinin (HA), the ubiquitous viral surface protein.[85,86] By extensive interaction and a steric shielding of the viruses by polymer systems, it has become possible to competitively suppress adhesion on the target cells.

In addition to these polyvalent viral inhibitors, ligands for cellular targets, for example, as membrane-bound receptors, have also been developed which are based on linear polymers. Some current examples are the multivalent ROMP-based (ROMP = ring-opening metathesis polymerization) linear polymers developed by Kiessling et al.[87] and the application of water-soluble polyacrylamides (*N*-(2-hydroxypropyl)methacrylate, HPMA) by Kopeček and co-workers.[88] Other important statistic multivalent scaffold architectures are glycopolymers,[89] which range from semisynthetic hybrids with varied sugar functionalization to natural structures with polydispersed chain lengths, such as chitosans, dextrans, heparins, and hyaluronic acids. Linear polymers (random coil) do not have an oriented ligand presentation, as—unlike

defined surfaces or globular structures—they can exhibit many different conformations. Dendritic polymers, on the other hand, already have a defined architecture and the highest conceivable surface functionalization. In the past, however, small defined multivalent dendrons and dendrimers have mainly been used.[90,91] Landers et al. have shown that a SA-conjugated polyamidoamine dendrimer (G4-SA) can be adapted to inhibit hemagglutination (an erythrocyte–virus interaction) in vitro when sialic acid is linked through a short spacer.[92] Interestingly, the incorporation of a longer PEG spacer to allow a more flexible exposure of SA at the dendrimer led to an unsuccessful inhibition. This finding indicates the importance of the spacer within the molecule and can be explained by the excessive flexibility of the system, which would result in a great loss of entropy as a consequence of multivalent binding. The active SA conjugate is also able to inhibit pulmonary influenza A infections in vivo. However, it has also been shown that adhesion blockages are virus-type-specific, which is due to the different accessibilities of the individual hemagglutinin binding sites. Although many approaches are based on small dendrimers, these low-valent structures (usually with $n = 4$–16) are noncompetitive in extensive interactions or interaction sites, since they are located far apart (see Section 4.3).

Recently Cloninger[93] as well as Hammond and co-workers[94] designed globular architectures with multivalent antennas. They used branched end groups to generate "clustered" ligands for better binding properties than statistically loaded surfaces.

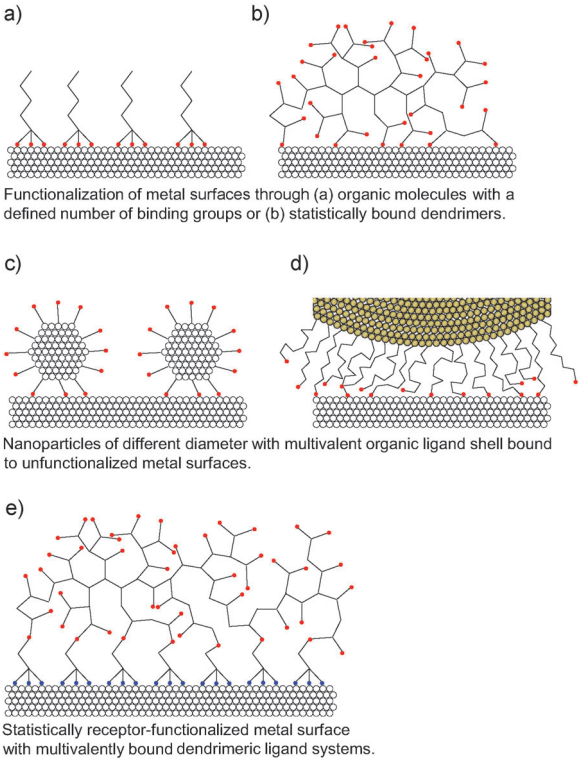

Figure 9. Various statistic multivalent binding modes between organic and inorganic binding partners for the formation of hybrid materials (see text for details).

3.1.2. Hybrid Materials

Organic materials can be linked in a variety of ways to inorganic materials through multivalent interactions to give new structures. Metallic or oxide surfaces in the form of extended surfaces or as nanoparticles primarily serve as the inorganic substrates. Other materials such as graphite and silicon are also used. A special case are three-dimensional networks (metal-organic frameworks, MOFs), which lack space for further internal functionalization (e.g. for ligands) and, therefore, have been used instead in materials science.[95] The organic reactant may be small organic molecules as well as larger systems of dendrimers, polymers, and biomolecules, such as DNA or proteins. Several statistical multivalent binding modes are possible between organic and inorganic materials (Figure 9).

On a not-further-functionalized metal, metal oxide, or graphite surface, in which only a small fraction of the atoms act as a binding partner, the link to the organic binding partner is statistical. In this case, the organic partner can bind itself with a defined number of functional groups, for example, with a bi- or trivalent thiol on a gold surface (Figure 9a)[67] or with substituted pyridines on graphite surfaces.[96] The organic partner may also be statistically linked, as in the binding of a dendrimer to a metal or glass surface (Figure 9b).[97] Zhou et al. used multivalently bound poly(amidoamine) dendrimers on a glass surface that were functionalized with terminal aminoxy and hydrazide groups for the controlled coupling of various mono-, oligo-, and polysaccharides.[97] Instead of an organic molecule, inorganic nanoparticles can also bind to a surface with an organic ligand shell, so that in such a hybrid material only the interactive material itself needs to be organic. In this case, practically all the nanoparticle ligands facing the substrate bind to the surface depending on the density, radius of curvature, and rigidity of the ligand, (Figure 9c), or there is only a statistical interaction with a few ligands (Figure 9d). An example is the interaction between silica particles functionalized with dithiocarbamates and a gold surface.[98] Alternatively, the surface of the inorganic substrate itself may be functionalized with organic ligands/receptors (e.g. thiols, DNA, proteins) which multivalently interact with an organic or nanoparticle binding partner (Figure 9e). As a rule, this link is statistical if the density of the surface-bound ligand is sufficiently high. The surface-bound ligands themselves can be multi- or monovalently bound to the inorganic surface.

Dorokhin et al. functionalized glass surfaces with a layer of β-cyclodextrins and attached a further layer of adamantyl-terminated poly(propyleneimine) dendrimers on top to bind β-cyclodextrinheptamine-functionalized CdSe/ZnS semiconductor nanoparticles.[99] Such multivalently stabilized layered structures are interesting for applications in optoelectronics[100,101] as well as in sensors.[102,103] Johnson and Levicky succeeded in irreversibly depositing thiol-terminated poly(mercaptopropyl)methylsiloxane (PMPMS) on a gold substrate[104] through a combination of the multivalent interaction of the thiol groups and the high hydrophobicity of the polymer. Thereafter, it was possible to covalently bond thiol-

terminated DNA oligonucleotides to the substrate. The resulting system is stable at temperatures of up to nearly 100 °C, which opens up new applications in diagnostics. It is also possible to build larger three-dimensional structures by multivalently linking nanoparticles on a planar surface (see Section 4.1). Inorganic–organic hybrid systems may also be produced in solution if they are not deposited on substrates. In these cases, the multivalent interactions induce a controlled aggregation of the reactants. Wagner et al. developed switchable and reversible colloid arrangements by using multivalent electrostatic interactions between gold nanoparticles and coiled-coil peptides.[105]

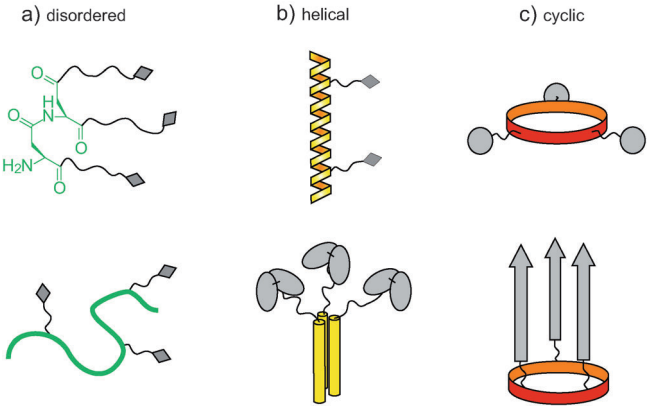

Figure 10. Various multivalent peptide scaffolds. a) Disordered structures: small trivalent scaffold β-DD with glycosyl ligands (top), linear peptide chain with side-chain-linked ligands (bottom). b) Helical structures: α helix with glycosyl ligands (top), trivalent collagen-based framework with three scFv ligands (single-chain variable fragments), (bottom). c) Cyclic structures: radial arrangement of the ligands (top) and an axial arrangement of the ligands, for example, β sheets (bottom).

3.2. Programmed Multivalency with Defined Biopolymers

Unlike the above-described synthetic polymer systems, which were formed from rational considerations about multiplicity, nature is able to create significantly more complex architectures with customized biopolymers (peptides, proteins, DNA).

3.2.1. Peptide-Based Scaffold Structures

A defined spatial orientation of carbohydrate moieties in synthetic glycopolymers is often difficult to realize. By using both short flexible and conformationally fixed model peptides, the role of a protein–substrate conformation in the glycosylation process has been explored using exactly positioned ligands, particularly for *N*-glycosylated derivatives.[222] The advantage of applying model peptides is that a variety of analytical methods can be used for structural characterization, and by comparing the glycosylated and nonglycosylated forms valuable information on the conformational consequences of modifications can be obtained.

A review of the various peptide-backbone-based multivalent structures will be presented with a few selected examples. The goal here is not a comprehensive listing of all the previously synthesized, peptide-based multivalent scaffold structures, but rather an overview of the geometric possibilities and a discussion of the differences.

Regarding disordered scaffold structures, there are a number of very different structures that fall under the category of disordered peptide-based scaffolds. In the most extreme cases, they have only one amino acid or they can consist of several hundred amino acids with an equal number of ligands. Lee and co-workers developed trivalent inhibitors based on γ-L-glutamyl-L-glutamic acid (γ-EE) or β-L-aspartyl-L-aspartic acid (β-DD) for the asialo glycoprotein receptor (ASGP-R).[106,107] In this case, GalNAc ligands were introduced to three carboxy groups of glutamic and aspartic acid, respectively (Figure 10a, top) through hydrophobic aminohexyl spacers. Tam developed so-called MAPs (multiple antigen peptides) based on the junction of lysine residues.[108,109] Since then, this concept has been used to synthesize and study a variety of multivalent peptide and glycopeptide dendrimers.[110,111]

Multivalent homopolymeric linear peptide chains are much more widespread than the above-described small scaffolds. A number of ligands are generally introduced and randomly distributed into the peptide chain through functional amino acid side chains. The best known example is poly-L-glutamic acid (PGA), to which the ligands are introduced in the carboxy side chains through chemical or chemoenzymatic techniques. Even wide gaps between the receptors can be bridged by the long linear polymer scaffold. In addition, the flexible structure allows a relatively tension-free interaction between the ligands and receptors. Other advantages of the PGA scaffold are its low toxicity and immunogenicity as well as good biodegradability and water solubility (10% w/v). Highly polymeric lysoganglioside–PGA conjugates have proven their worth as picomolar inhibitors of the trimeric hemagglutinin of the influenza virus.[112] Both the molecular weight of the PGA as well as the ligand concentration parameters influence the binding effectiveness of influenza viruses by PGA-based polymers.[113] When the ligand densities are too large, the binding is adversely affected, probably for steric reasons.[114] Introduction of aminohexyl spacers between the PGA backbone and the ligand should remove the steric constraints.

PGA-based glycopeptides also selectively bind with numerous plant lectins.[115,116] The glycosylated PGA backbone is, therefore, suitable as a model system for glycans of the mucin type.[116] The glycopeptides specifically interact with the corresponding lectins, regardless of how much the glycan sugar residues have been truncated to more simple glycans compared to the natural glycoprotein.

Small amino acids, such as glycine or alanine, with side groups that show the least influence on the solubility on the whole construct can serve as spacers between the functionalized amino acids. Thus, not only the distance between the ligands but also the secondary structure of the peptide can be influenced. These systems are ideally suited for investigating the influence of the ligand distance upon ligand–receptor interactions. Unverzagt et al. synthesized a series of divalent

model peptides as inhibitors of the influenza virus.[118] In this case, sialyl *N*-acetyllactosamine ligands were linked to asparagine units, which again were interconnected with flexible glycine fragments of different chain lengths.

With regard to helical backbone structures, polypeptides, which are mostly constructed from amino acids such as alanine or proline with a strong propensity for helix formation, can act as helical, multivalent peptide backbone structures. They are considerably stiffer than disordered structures, which means the ligand distances have to be better adapted to the receptor distances along the helix axis. At the same time, the loss of entropy is also reduced during the ligand–receptor interaction.[117]

Unverzagt et al. used a divalent system for influenza inhibitors to study the relationship between the length of the proline chain between the ligands and the effectiveness of inhibition.[118] If the two ligands were unfavorably placed along the rigid proline helix, then the inhibition was worse than a monovalent system. For their systematic study, Liu and Kiick used an alanine-rich sequence as an α-helical backbone structure for cholera toxin inhibitors.[119] The glycosyl ligands were linked to glutamate side chains on the peptide backbone through aminohexyl spacers so that they were positioned at different distances from each other. The α-helical inhibitor Cap 35-H-6 showed approximately twice the inhibition than the disordered multivalent inhibitor Cap 35-RC-6, probably because of the smaller loss of conformational entropy (Cap 35-RC-6: 162-fold higher inhibition, Cap 35-H-6: 340-fold higher inhibition compared to monovalent ligands).

Falenski et al. recently showed that the α-helical coiled-coil folding motif is an appropriate multivalent scaffold structure for presenting several glycosyl ligands along the helix axis.[120] As a result of its typical primary structure with a repeated heptad pattern, the helical coiled-coil system offers unique opportunities for an adjustable presentation of carbohydrate functionalities. Within the coiled-coil folding motif, 2–7 α helices wind around each other in a left-handed arrangement (Figure 11). The thermodynamic driving force for the aggregation of multiple peptide helices is mostly achieved by arranging hydrophobic amino acids at positions a and d to a hydrophobic core. The positions e and g, which are often occupied by charged amino acids such as lysine or glutamate, influence the specificity of the folding (parallel versus antiparallel) through electrostatic interactions. The positions a, d, e, and g can thus be summarized as an interhelical recognition domain (Figure 11). Positions b, c, and f of the heptads repeated pattern are exposed to the solvent on the surface of the helical cylinder (Figure 11). They can be used either alone or in combination to install carbohydrate building blocks, which allows a fine-tuning of the distance of the building blocks. A gradual, but relatively small destabilizing of the coiled-coil structure was observed when the glycosyl ligands were introduced. Even the introduction of 12 β-D-galactose residues (6 β-D-galactose residues per 26 amino acid long peptide) on the serine side chains in the solvent-exposed positions of a coiled-coil dimer resulted in a stable coiled-coil structure ($T_m = 72\,°C$ compared to 85 °C for the unglycosylated peptide). The interaction of coiled-coil glycopeptides with natural glycoprotein receptors, such as

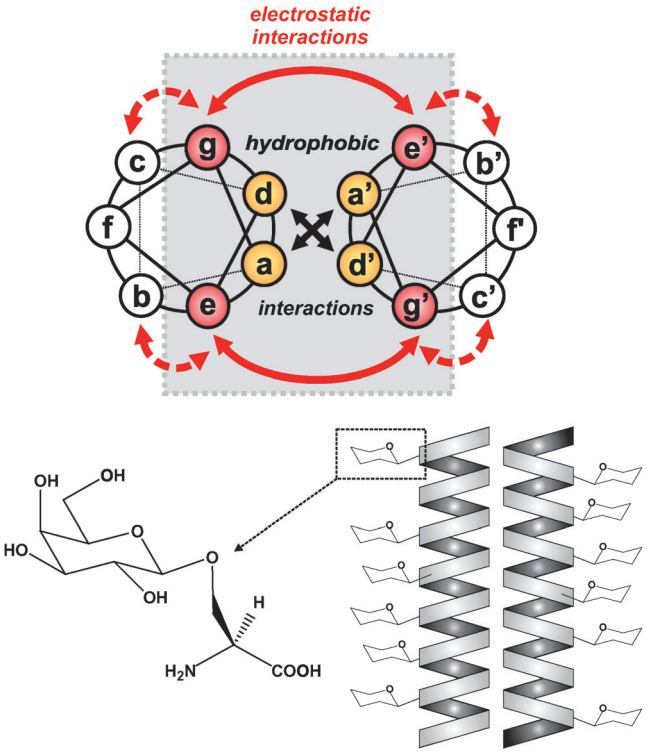

Figure 11. Top: helical-wheel representation of a parallel coiled coil dimer. Bottom: schematic representation of an α-helical coiled-coil dimer hyperglycosylated in positions b, c, and f.

lectins and the asialoglycoprotein receptor of HepG2 cells, is currently being tested in further studies.

Some advantages of using peptide-backbone-based scaffold structures are that they are accessible by chemical solid-phase peptide synthesis and established orthogonal protecting-group strategies. Larger peptide-backbone structures are accessible by chemical ligation, polymerization, or expression. Various side-chain functionalities of amino acids allow an easy introduction of different ligands, and monodisperse systems are obtained by targeted introduction of the ligands. Peptide scaffolds that are based on helical systems or cyclopeptides enable the distance between the ligands to be controlled. Furthermore, they are adapted by nature and, therefore, biocompatible, which means they have low toxicity and immunogenicity in addition to being water-soluble and biodegradable. Whether the good biodegradability by proteolysis is disadvantageous largely depends on the context in which the peptide-based multivalent systems are to be used and whether they are random or disordered, definitively folded, or if they are highly organized systems. The synthesis of long peptide sequences is sometimes difficult and generally relatively expensive. This disadvantage can be overcome in several cases with self-organization processes. Since longer receptor distances must be bridged with longer and more-flexible peptide sequences, it may be difficult to control the distances between the individual ligands and thus minimize the loss of conformational entropy on binding to the receptor. Furthermore, the amino acid side chains offer additional

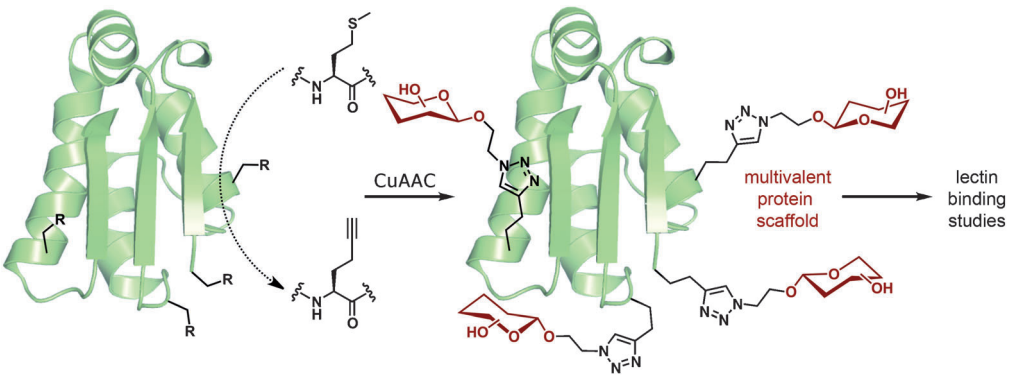

Figure 12. Use of a barstar protein as a multivalent scaffold.[121] The alkyne functions were introduced at specific sites by substitution of a canonical amino acid (methionine) with homopropargylglycine. CuAAC: Cu-catalyzed azide-alkyne cycloaddition.

functionalities with which the receptor molecules might be able to interact. This interaction could be enhanced by the correct design.

Recently, several bioorthogonal functionalities were directly targeted to whole proteins by site-specific mutageneis and genetic code engineering.[121] As a result, tailored multivalent biomolecules have been generated by established conjugation methods for efficient lectin inhibition (Figure 12).

3.2.2. PNA/DNA

Nucleic acid molecules are no longer considered to be just genetic storage material and are now regarded as structure templates. The Watson–Crick base-pairing rules are being used to prime DNA and RNA molecules as well as analogues to form well-defined architectures in regard to their structure and size.[122,123] Duplex, triplex, and, recently even quadruplex structures have been prominently used to arrange chromophores,[124] metals,[125,126] and even proteins[127] at exactly set intervals. As a result, the majority of work in this area has addressed materials science problems.

Lately, researchers have noted that architectures based on nucleic acids open the door to fascinating possibilities for molecular life sciences.[128,129] Thus, the use of nucleic acid architectures for multivalent ligand presentation are especially interesting because:

a) monodisperse materials can be chemically or biologically synthesized virtually on any length scale,
b) the valence of a ligand is controllable by sequence-instructed self-assembly, and
c) the functional groups on the nucleic acid helix can be positioned with Angström accuracy.

Another advantage is that the rigidity/flexibility of nucleic acid architectures can be selectively adjusted. Thus, a DNA double strand can have a persistence length of 500 Å, in which case, the DNA duplex behaves as a rigid rod.[130,131] Most rod structures tend to aggregate. In contrast, DNA duplex architectures are characterized by their high water solubility, which is a very important feature for biological studies. The flexibility of the nucleic acid scaffold can be gradually increased by stepwise incorporation of single-strand breaks or single-stranded segments.

Kobayashi and co-workers introduced oligonucleotide–monosaccharide conjugates with half-sided complementary sequences for oligomerization through hybridization.[132–135] The resulting DNA–galactose or DNA–mannose clusters are characterized by a strict periodicity of the saccharide presentation. These structures have been used to show that the helical torsion of the ligand presentation in a DNA duplex affects the cooperative binding of lectins. Three monosaccharide ligands were required for a multivalent interaction with lectins, such as Ricinus communis agglutinin or concanavalin A.

Winssinger and co-workers described a method in which the topology of a triantennary oligomannoside that was recognizable by the HIV-neutralizing 2G12 antibody could be mimicked by an adjacent presentation of two simple mannosides.[136] In this case, di- and trimannose units were coupled to the N- (5′) or C-terminal (3′) ends of peptide nucleic acids (PNAs). PNA is a non-ionic DNA analogue that forms very stable, double-helical structures with complementary DNA or RNA strands. A similar approach was used by Winssinger and co-workers for a divalent presentation of cyclopeptides.[137] By using PNA–PNA hybridization, the resulting dimerized PNA–cyclic peptide conjugates showed a tenfold higher affinity than monovalent conjugates for the cytokine receptor DR5.

Scheibe et al. showed that PNA–sugar conjugates can be used for measuring the distances of binding sites in *Erythrina cristagalli* lectin (ECL).[68] Only five different PNA conjugates were needed to develop a variety of multivalent architectures by permutation of complementary sequences on the DNA template. Apella and co-workers recently used this method to construct a high-affinity binder for integrins. The latter mediate cell–cell adhesion, and overexpression of these multivalent receptors has been connected to cancer metastasis. The best constructs carried 20 cyclopeptide ligands and showed, both in vitro and in vivo, a twofold better binding inhibition of melanoma cells on the extracellular matrix compared with monovalent cyclic peptides.[138]

Eberhard et al. decorated DNA architectures with phosphopeptide ligands and used divalent conjugates to spatially screen the tandem phosphopeptide binding domains of Syk kinase.[139] In this study, single-stranded segments were included in the architectures to gain more information on the flexibility of a protein domain. Abendroth et al. conducted similar studies on the estrogen receptor (see Figure 14 in Section 3.2.3).[140] The spatial screening, which was programmed with DNA, gave the distance of the consensus binding pockets for estrogen, and indicated that there was an

additional hydrophobic binding site on the surface of the ligand binding domain.

The research groups of Neri and Hamilton described self-assembled, DNA-encoded libraries, in which small molecules were bound to oligonucleotides in order to bi- or trivalently present them after hybridization on the ends of duplexes and triplexes.[141–143] This method should make it easier to identify drugs for medical applications. Terminally modified templates based on a DNA quadruplex structure now make it possible to control the affinity of the presented ligands for target proteins such as cytochrome *c* or trypsin.[144–146]

Winssinger and co-workers made use of an adjacent hybridization of PNA conjugates with DNA templates. One example showed that 62500 combinations of small-molecule ligands allowed, after affinity selection against carbonic anhydrase, a partial convergence within a carboanhydrase inhibition library.[147] Chaput and co-workers used the heterodivalent presentation of peptides on DNA duplexes to construct a high-affinity binder for a regulatory protein Gal180 of yeast.[148]

3.2.3. *Spatial Screening for Measuring Distances in Protein Complexes*

One of the advantages of DNA architectures is that the distances between the presented ligands can be programmed for wide areas through the sequence of the participating strands. In the following examples, the ligands are presented at intervals of between 3 and 150 Å to measure the distance between the binding sites in the receptors. In particular, multivalent interactions between proteins and carbohydrates, small molecules, and proteins will be considered. Theoretical preconsiderations of flexible and rigid spacers can be found in Section 2.

For the spatial screening of *Erythrina cristagalli* lectin (ECL), Scheibe et al. synthesized PNA–LacNAc conjugates.[68] Altogether, five different PNA oligomers were prepared that covered three independent anticodon sequences. In principle, a DNA template which contained three different codon segments at four positions allows formation of 324 supramolecules (Figure 13). A tetravalent PNA–DNA complex was bound by ECL with a more than 700-fold (180-fold per ligand) higher affinity than a monovalent PNA–DNA complex. The highest affinities were measured in divalent complexes when the LacNAc ligands were arranged at a distance of 104 Å. The insertion of single-strand segments between the two double-helical regions in **III** resulted in even higher affinities. The distance between opposing binding sites in a homodimer of ECL was found to be 65 Å. The authors concluded that divalent ligands had to adjust the curvature of the protein surface, which was easiest if the ligands were provided by a flexible template with a linear distance of 100 Å.

Many proteins that are involved in the formation of protein–protein interaction networks have several protein-binding domains. Without knowledge of the protein's structure, it is difficult to quantify the conditions for the high-affinity binding of a specific substrate. Eberhard et al. used DNA–peptide conjugates to estimate the distances between

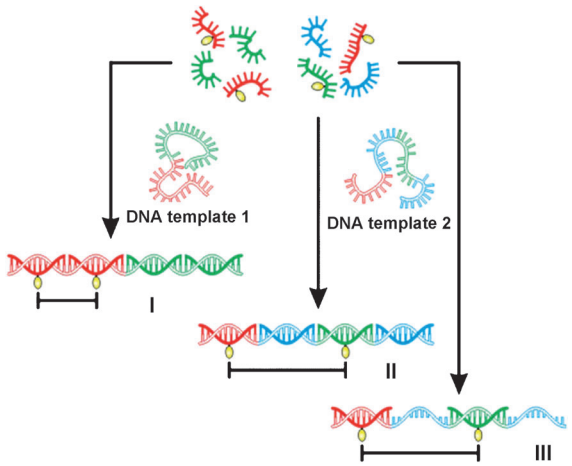

Figure 13. Sequence-programmed formation of PNA–DNA complexes for control of the valence (not shown), and spatial distribution of glycoligands (yellow).

the tandem SH2 domains of Syk kinase, an important signaling enzyme in the activation of B lymphocytes.[139] SH2 domains bind peptide motifs that contain phosphotyrosine and are conjugated with cysteine-modified oligonucleotides through a maleinimidyl unit. In this study, several DNA architectures were examined (Figure 14). Divalent single strands **1** bind to the Syk-tSH2 domain with very high affinity, with the distance between the phosphopeptide anchor not playing a role. The authors attributed this behavior to the high flexibility of single-stranded DNA. Rigid duplexes **2** were

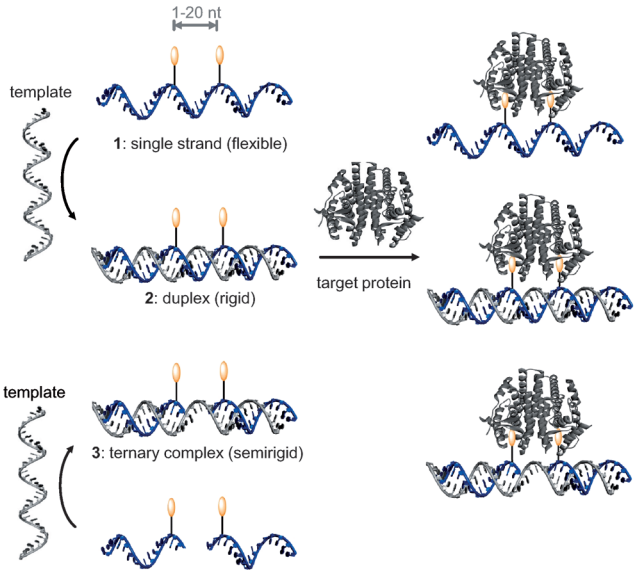

Figure 14. The principle of spatial screening of proteins with divalent peptide–DNA complexes as flexible single strands (**1**), rigid double strands (**2**), and including single-stranded segments in semi-rigid ternary complexes (**3**). Tandem SH2 domains of Syk kinase were systematically investigated in all three modes with KpYETLG motifs containing phosphotyrosine.[139] A spatial screening of the estrogen receptor with estrogen analogues in ternary complexes showed the distance between the consensus binding sites and even indicated a second hydrophobic binding site.[150] nt = nucleotide.

formed after hybridization with a complementary DNA strand. Duplexes, in which the phosphopeptides were arranged at a distance of 5 or 16 nucleotides on opposite sides of the double helix, showed low affinity for Syk-tSH2. The highest affinities were observed when the phosphopeptides were positioned on the same side of the helix at a distance of 2 nucleotides (≈ 7 Å) or 11 nucleotides (≈ 37 Å), but not 21 nucleotides (≈ 70 Å). The authors concluded that the interdomain connecting the two SH2 domains in the Syk kinase was not in a position to span distances of 70 Å. The helical twist makes distance measurements more difficult between 10 and 25 Å, as well as for all the integral multiples. For this reason, the authors added single-stranded regions between the duplex segments of the ternary complexes **3**. FRET measurements show that these regions do indeed have rotational degrees of freedom, but are still significantly lower than fully flexible unpaired single strands. Experiments with ternary complexes **3**, in which the unpaired regions were extended stepwise, suggest that the Syk interdomain is sufficiently flexible to arrange the SH2 domains at intervals between 7 and 50 Å.

Another recent example is an investigation of divalent interactions within the homodimeric estrogen receptor with a receptor spacing of 3.9 nm (Figure 14), in which the crystal structure in the presence of different ligands as well as the first divalent ligands with flexible spacers were reported.[149] The new challenge was then to develop a molecular scale for elucidation of unknown quaternary structures in protein complexes based on rigid DNA spacers. In fact, the custom-made rigid DNA spacer provided the highest binding affinity compared to short or over-long DNA spacers.[150] Even flexible synthetic PEG spacers only showed a relatively weak divalent binding.[149]

Wittmann and co-workers showed by an X-ray structure analysis of a lectin–ligand complex (WGA-GlcNAc) that wheat germ agglutinin (WGA) has four binding domains with a total of eight binding sites, whereby two neighboring binding sites in the crystal structure could each be occupied and thus bridged by divalent ligands.[151] This structure was confirmed in solution by EPR spectroscopy. Moreover, *N*-acetylglucosamine ligands could be bound through PEG spacers of different lengths and marked with terminal spin probes. The distance distribution of the divalent ligands could thus be measured at different ligand/receptor ratios with these divalent constructions. With this method, the optimal binding distance between two ligands in solution and a variety of binding modes could also be determined.[76]

4. Function of Multivalent and Polyvalent Systems

After a discussion of the basic principles of multivalency and various scaffold architectures, functional multivalent and polyvalent systems will be presented in this section. For the most part, they are biologically inspired examples with applications in medicine, but a number of interesting supramolecular systems have also recently been developed.

4.1. Artificial Supramolecular Systems

Defined supramolecular systems that are based on inorganic, organic, or biological chemistry are especially valuable for understanding the forces involved in multivalent interactions and processes in solution. If they can also be integrated in targeted modeled and synthetically built planar or spherical nanostructures with a defined surface, quantitative studies of numerous comprehensive multivalent effects should be possible, as they arise, in particular, at large interfacial areas (polyvalence).

Although there are many synthetic multivalent hosts and guests in supramolecular chemistry, there are surprisingly few studies that attempt a detailed description of the thermodynamics and kinetics. Some general models for self-organization processes[152,153] have been accompanied by concrete models, such as for the self-assembly of meso-pyridyl-zinc-porphyrins into tetramers.[154] Melamine cyanurate rosettes,[155,156] in which a larger number of blocks were brought together by hydrogen bonds to form a complex, have been investigated in terms of the entropic contributions to the binding.

In addition to the examples of detailed thermochemical analysis of the systems shown in Section 2.3, a number of other cooperative and multivalent binding processes have been reported, such as in the early work of Lehn and co-workers on transition-metal helicates,[157–160] the porphyrin ladders of Taylor and Anderson,[161] as well as the oligoamide molecular zippers of Hunter and co-workers[162,163] (Figure 15).

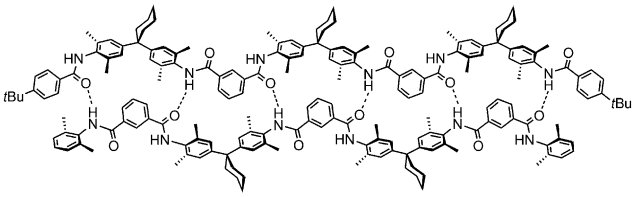

Figure 15. A positively cooperative oligoamide zipper binding.

The binding energies increase exponentially upon systematically varying the length of the mutually complementary components from two to six hydrogen bonds. Each additional hydrogen bond thus provides a higher energy than the previous one.

A number of publications have discussed the role of the spacer and its flexibility. Already in the early 1970s, Page and Jencks estimated the entropic cost of a fixed but previously freely rotatable C–C bond to be $-T\Delta S = 3.8\ \mathrm{kJ\,mol^{-1}}$ (CH_2–CH_2) and $-T\Delta S = 7.5\ \mathrm{kJ\,mol^{-1}}$ (CH_2–C=O) at room temperature.[164] Searle and Williams reported slightly smaller values of $-T\Delta S = 1.6$ to $-3.6\ \mathrm{kJ\,mol^{-1}}$ at 300 K for fixing rotors in hydrocarbon chains during the crystallization of an alkane.[165] Later, Schneider and co-workers found that a series of divalent bisamide/biscarboxylate complexes with spacers of different lengths had a value of $-T\Delta S = 1.3\ \mathrm{kJ\,mol^{-1}}$.[166,167] These studies showed that the advantage of synthetic model

systems is that they can be systematically changed to allow precise predictions about the thermochemical parameters.

Binding enhancement has also been found in complexes of modified peptides with cucurbit[8]uril (Figure 16).[168]

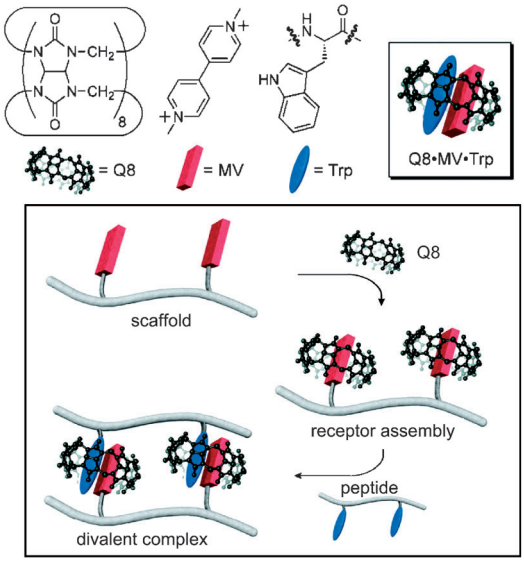

Figure 16. Cucurbit[8]uril (Q8) forms ternary complexes with methylviologen (MV) and electron-rich aromatic compounds, for example, with the side chain of tryptophan (Trp). The peptides can be programmed with these two guests to easily generate multivalent host–guest complexes (bottom). Reproduced from Ref. [168] by courtesy of the American Chemical Society.

Cucurbit[8]uril can bind two guests in its cavity simultaneously, whereby one of them tends to be a dication with a length corresponding to the distance between the two inwardly facing carbonyl groups of the cucurbit[8]uril barrel. Methylviologen is an example of an electron-deficient guest that assists the taking up of additional electron-rich aromatic compounds as a complementary guest in the cucurbituril cavity. If a peptide is functionalized with viologen side chains and a second peptide with tryptophan at the same intervals, the two peptides form a double strand upon addition of cucurbit[8]uril as a result of the pairing of the complementary guests. Depending on the number of interactions possible, this can also result in multivalent complexes, for example, a trivalent one that has an up to 210 times higher binding constant than a corresponding monovalent aggregate.

The complexity may be reduced even more, if the supramolecular complexes are examined in the highly diluted gas phase by mass spectrometry. This eliminates the solvent effects totally and allows investigation of the intrinsic properties of a complex. Thermochemical analysis in the gas phase is very complex and has not yet been performed for multivalent systems, but Armentrout has already been able to determine the binding energies of the crown ethers [12]crown-4 to [18]crown-6 and of the other ethers to alkali metals.[169] One of the key findings in these studies was that the binding energy values of the crown ethers were lower than the sum of the binding energies of a comparable number of short linear ethers with the same total number of donor atoms, because of the chelation effect. This means that the interactions of the crown ethers were systematically negatively cooperative. The generally accepted idea that alkali metal ions bind most strongly to crown ethers, whose cavities have the most accurate fit possible, is not nearly so clear in binding energies measured in the gas phase, compared to studies in solution (see Ref. [170] and references therein). This difference, which is attributable to a significant solvation effect, impressively shows that a comparison of isolated systems in the gas phase with experimental data from the condensed phase gives profound insight into solvation effects, and thus a more exact understanding of binding processes. Since this is particularly true for studying multivalent binding processes in which entropic effects may be relevant, interesting research results can be expected in the future.

To conclude this section on supramolecular multivalent systems, an example will be discussed in which multivalent binding results in a special function. After the synthesis of several trivalent so-called "super bundles",[171,172] Stoddart and co-workers built molecular elevators (Figure 17) by

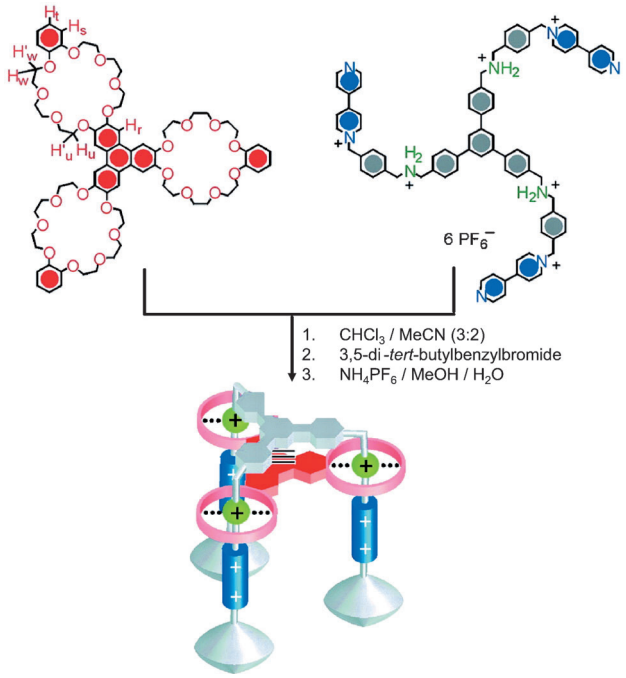

Figure 17. Synthesis of Stoddart's molecular elevator. Reproduced from Ref. [173] by courtesy of the AAAS.

attaching a viologen station (4,4′-bipyridinium) to each of the three ammonium arms of the guest component.[173,174] The [3]rotaxane resulting from attaching the stoppers was then switchable. If the secondary amines were protonated, the crown ether preferred to complex at these stations and the platform was located directly adjacent to the spacer of the guest. If deprotonated, the crown ether migrated to the viologen stations, thus reversibly "walking" along the trivalent ligand system and leading to an adjustable distance between the central aromatic scaffolds ("up" and "down").

A related kinetic study demonstrates the importance of comprehending the properties of the spacer for a deeper understanding of multivalency.[175] A viologen/dibenzo[24]crown-8 template can be used to successfully triple thread the three-armed viologen guest in the trivalent crown ether host (Figure 18). The first two threading steps are fast, but it takes

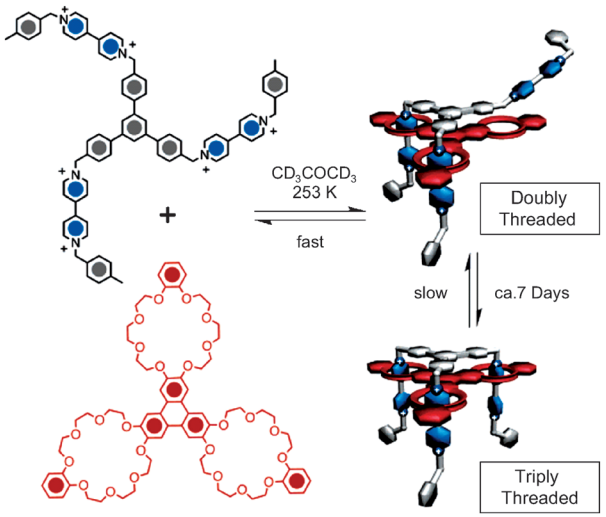

Figure 18. A triple-threaded pseudorotaxane based on a viologen/dibenzo[24]crown-8 template shows that multivalency may also be seen in kinetic parameters. Although the first two threading steps can occur very quickly, the third axis requires about 7 days for threading. Reproduced from Ref. [175] by courtesy of the American Chemical Society.

several days for the final, considerably slower third step to finish threading. The reason clearly lies in the chemical structure of the two components, which have rigid aromatic spacer scaffolds to which the binding sites are attached. Additionally, π–π interactions between the two scaffolds are possible. After the second threading, the complex is so rigid that the third threading has to overcome a high activation barrier. This example shows that the influence of a spacer is manifold and that a careful investigation of its influence must be done before multivalency effects can be fully understood. Treatment of just the thermodynamics in a multivalent interaction is too limited, because multivalency can clearly play a role in reaction kinetics.

Furthermore, multivalent supramolecular interactions can be applied to nanostructures on surfaces and for building new materials (see Section 3.1.2). Multivalent interactions on surfaces are used in biology and are more appropriate for initial and reversible immobilizations of larger objects such as whole cells and pathogens. Unlike most biochemical examples, supramolecular systems are superior for a basic and quantitative understanding of multi- or polyvalent interactions on surfaces because of their better defined structures.[153,176,177] More and more methods are being developed to use nanostructured surfaces or self-assembled monolayers (SAMs) for potential applications in the relevant size range of 1–100 nm.[178,179] Biologically or catalytically active, spatially defined, and thus addressable surfaces are particularly interesting.[180] Traditional lithographic processes with their technologically limited size scale of >100 nm were expanded to archieve even smaller structural sizes (nanolithography).[181]

It is also possible to create self-sorting and correcting planar as well as three-dimensional functional structures (or to alternatively selectively apply them to a surface substrate) by a multivalency-controlled self-assembly of supramolecular molecules or functionalized nanoparticles, as Reinhoudt, Huskens, and co-workers have demonstrated with several examples.[182] Crespo-Biel et al. reported an interesting example of a regular multilayer structure of multivalent guest–host interactions by alternating adsorbing adamantyl-presenting poly(propyleneimine) dendrimers and cyclodextrin-coated gold nanoparticles on an initial cyclodextrin SAM on gold surfaces (see Figure 19).[183,184] This approach makes it possible to build defined structured and stable surfaces as well as materials.

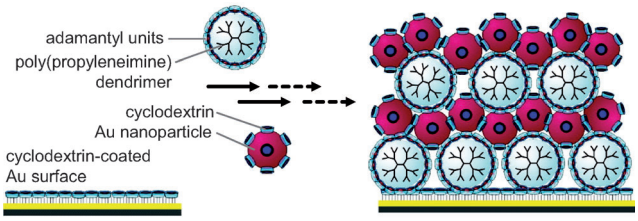

Figure 19. Building of three-dimensional structures by absorbing layers (layer-by-layer) of complementary functionalized, multivalent nanoparticles (PPI dendrimers and Au nanoparticles) on SAMs. Reproduced from Ref. [183] by courtesy of the American Chemical Society.

4.2. Multivalent Interactions on Biological Interfaces

Multi- and polyvalent interactions between lectins and glycans are of fundamental importance for the interaction of biological surfaces. Lectins are proteins with defined glycan-recognition domains on the surface of viruses and bacteria as well as of plant and animal cells. Affine inhibitors of lectins are, therefore, suitable for clarifying the function of defined carbohydrate structures, when they are used as a competitive binding partner. They also provide an opportunity for pharmacological intervention. The phenomenon of multivalent lectin–glycan interaction, which has been commonly referred to and described in the glycosciences as a glucoside cluster effect, emphasizes the special biological relevance of this system.[185] Multivalent glycan conjugates are referred to in this context as a glycan cluster (see dendrimer glycoclusters and DNA clusters in Sections 3.3.1 and 3.2.2, respectively).

The binding of an individual lectin to a glycan (monovalent bond) is relatively weak, with the dissociation constants (K_D) typically in the millimolar range. Stronger interactions occur if both binding partners develop clusters, whereby either several complementary, monovalent functionalities are presented on the interacting cellular surfaces (multivalent surfaces) or the multivalent interaction between two molecules occurs because of multiple presentations of functionality within the molecule (multivalent mole-

cule).[186,187] An interesting example of the latter case, the interaction of a monomolecular, multivalent receptor with a multivalent ligands, is the soluble bacterial adhesive cholera toxin (CT), which belongs to the AB_5 toxin family (Figure 20).

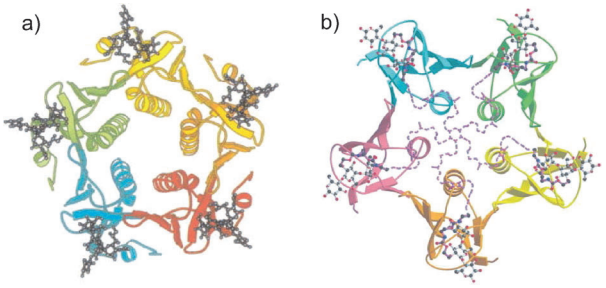

Figure 20. a) Crystal structure of a pentavalent cholera toxin B subunit bound to five GM1 pentasaccharides.[188] b) B_5 subunit of a shiga-related bacterial toxin bound to a pentavalent, star-shaped, synthetic polysaccharide inhibitor.[189] Reproduced with kind permission from Macmillan Publishers Ltd.

It consists of a toxin subunit that is solely responsible for the disease pattern (diarrhea) and five lectin subunits that allow cellular uptake in the intestinal enterocytes. Once CT has been organized in a pentavalent structure it binds ganglioside GM1 through its cellular ligands and is taken up endocytotically. This is a good model for studying the design of multivalent ligands because up to five ligands can bind to the cholera toxic. In this example, the addressable binding sites are clearly defined by their distance from one another.

The saccharide structure of the ganglioside GM1 consists of a pentasaccharide, whereby the terminal galactose and sialin acid units contribute almost entirely to the binding energy.[190] An interesting example of designed CT inhibitors that takes into account the significance of the spacer length and flexibility shows impressive, achievable increases in inhibition.[191] The individual lectin binding sites could be addressed here through multivalency. A divalent GM1 conjugate already produces a 9500-fold inhibitory effect (IC_{50}) compared to monovalent GM1 (based on the number of ligands per conjugate, this is nevertheless still 4750-fold stronger). An octavalent GM1 conjugate is even more effective with its 380000-fold inhibitory effect, in other words, 47500-fold more active per ligand. In addition to full occupation of all the binding sites, the aggregation of cholera toxins themselves also contributes to the inhibition through the multivalent ligands.[192]

In a similar manner, competitive binding assays are often carried out for the evaluation of effective inhibitory interactions, which ultimately generate an IC_{50} value, that is, the concentration of a drug that leads to a half-maximal inhibition of a protein/enzyme. This is a general problem in many biochemical measurements. These measurements are performed on a defined protein–ligand pair and thus give information not about affinities or binding constants, but on a correspondingly defined effect (in this case, inhibition). One can, therefore, only compare IC_{50} values within a given system with each other and not with binding constants of a protein–ligand system. Consequently, the multivalent ligand presentation leads to lower IC_{50} values, but a cooperative effect is usually not definable.

A strong inhibition of the CT–GM1 interaction can also occur when the inhibitor simply consists of galactose ligands instead of the complex pentasaccharide unit. The terminal galactose of the pentasaccharide is bound deep in the binding pocket of the CT and can, therefore, serve as a simple minimal ligand. For the design of an effective galactose-based inhibitor, it is therefore even more important for the gap between the hydrophilic binding pocket and the protein surface to be exactly spanned with a hydrophilic PEG spacer. In comparison to a GM1 dendrimer with the same structure, however, a galactose dendrimer[193] results in a much lower inhibitory potency that does not even reach the value of the monomeric ganglioside GM1. Its mode of action, however, underscores the general concept of a binding enhancement by multivalent ligand presentation.

Another well-studied example of strong lectin–glycan interactions between polyvalent surfaces are selectins and their glycan ligands. In this cell–cell interaction, selectins and ligands, which are presented on both surfaces, initiate the adhesion of leukocytes from the blood to the vascular endothelium. This leads to the extravasation of leukocytes into the inflamed tissue (Figure 21). In pathophysiological situations, this extravasation is deregulated and the massive infiltration of leukocytes amplifies the inflammatory response with increased tissue damage.

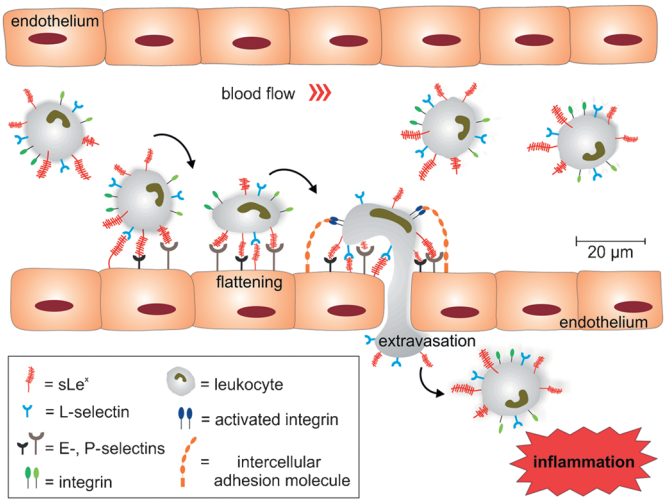

Figure 21. The selectin–ligand interaction recruites leukocytes to the vascular endothelium, which allows them to adhere. Following the inflammatory mediators, leukocytes migrate from the blood vessels towards the focus of inflammation.

Selectins are C-type lectins that form calcium-dependent bonds with their physiological ligands. The leukocyte L-selectin and the E- and P-selectins presented on the endothelia recognize all the sialyl Lewis^x tetrasaccharide ligands (sLe^x, Figure 22) that are presented by membrane-bound proteins or lipids on both interacting cellular surfaces (Figure 21). Additional sulfation of the ligand is a modifica-

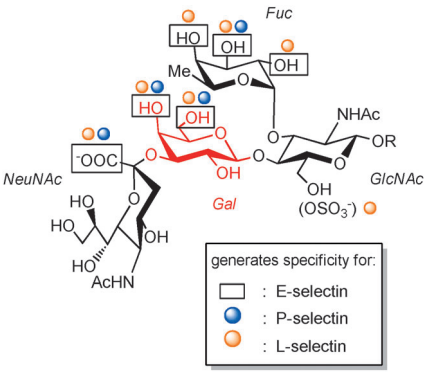

Figure 22. Structure of a sialyl Lewis^x ligand (sLe^x) und its selectin-specific detection capabilities.

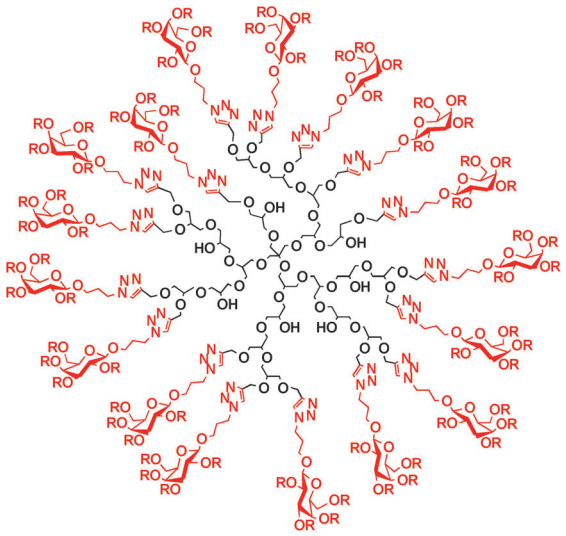

Figure 23. Schematic structure of a dendritic galactose conjugate with high L-selectin binding; $IC_{50} = 2.45$ μM (R=H) and 35 nM ($R = SO_3Na$).

tion that further enhances the binding of L- and P-selectin. The monovalent selectin–sLe^x interaction is weak and has a K_D value in the mM range. In a reductionist approach, the leading structure sLe^x could be successively simplified, and sLe^x mimetics could even be generated by using partial structures with only one glycan (fucose, galactose, sialic acid, and others). Although these monovalent building blocks show poorer affinities to the selectins, their activity could also dramatically increase by *n*-valent presentation; however, relatively low-valent systems ($n < 10$) have been examined in most cases.[194–196] Investigations of polyvalent systems that help strengthen this interaction with their two-dimensional interfacial character (similar to the zipper) have been very important. Such polyvalent selectin inhibitors could hinder the building of conformed cell junctions far more efficiently and should, therefore, be suitable for reducing the inflammation.[197,198]

Thoma et al. were able to show that linear polylysine polymers conjugated to a sLe^x analogue could dramatically reduce the E-selectin-mediated cell–cell interaction under physiological flow conditions.[199] While the monovalent ligand had an IC_{50} value of 30–40 μM, a functionalized polymer decorated with 420 ligands gave an IC_{50} value of 50 nM, based on the ligand concentration at the polymer. The multivalent presentation of just the E-selectin ligand alone increased the inhibitory effect of a single ligand by a factor of 700. The authors could further show that the size and the degree of the polymer's functionalization are crucial for the inhibitory effect and lead to a high loading density which sterically hinders the interaction.

In studies on selectin inhibition with functionalized dendritic glycopolymers (Figure 23) Papp et al. could demonstrate with a competitive SPR-based measurement system that galactose acts as a minimal selectin ligand, if available in sufficient concentration.[200] Compared to a tetravalent architecture ($IC_{50} = 240$ μM), a dendritic polyglycerol–glycan conjugate with 35 galactose units effected a 100-fold strengthening of the L-selectin ligand inhibition, based on a single galactose unit ($IC_{50} = 2.45$ μM). The additional introduction of sulfate groups into the galactose conjugate enhanced the inhibition by a factor of 70, and an IC_{50} value of 35 nM was reached. This clear evidence of a multivalence effect can still be significantly improved upon by using a rigid scaffold architecture (see below).

Analogous to the sulfated multivalent glycoconjugates, the dendritic polyglycerolsulfate (dPGS), which binds in the nanomolar range to L- and P-selectins, as well as to other inflammatory mediators, was identified to be a highly active anti-inflammatory compound (see Section 4.3).[72,201,202]

Even if the presentation of the ligands on a spherical or planar polymer surface cannot be rationally coordinated to the complementary receptor positioning but is statistically distributed instead (see Section 3.1), the result is a significantly higher inhibition that can now be reconciled with theoretical methods in terms of binding kinetics (e.g. possibly increased rebonding of the ligands) and better thermodynamics.

In addition to the polyvalent surface interactions of nanoparticles with planar material surfaces, as described in Section 4.1, the interactions of nanoparticles with biological surfaces are very important, especially for imaging and diagnostics. Multivalent interactions play an important role in two ways in the production, stabilization, and application of inorganic nanoparticles: First, the strength of both the nanoparticle–ligand binding and its stability can be considerably increased by the multivalent binding of organic ligands to nanoparticles compared to other reagents. At the same time, the aggregation in a dispersion can be significantly diminished because of a lack of steric or electrostatic stabilization. On the other hand, the nanoparticles that have been functionalized with organic ligands are a multivalent system themselves if the end groups of the ligands carry functional groups. Some advantages of nanoparticulate systems are that many functions are located on such a carrier in a confined space so that multivalent enhancement effects are possible without a substantial loss of conformational entropy. Additionally, in contrast to extensive, multivalent functionalized surfaces on bulk substrates, nanoparticulate carriers are mobile in emulsions. Furthermore, the shape, size, and

physical properties of these particles can be selectively adjusted and the multivalent functional groups can be coupled with properties such as fluorescence or magnetism if a suitable core is selected.[203] These unique combination possibilities make multivalent functionalized nanoparticles attractive systems for numerous applications in the life sciences. An example is the glyconanoparticles developed in 2001 by Penades and co-workers with carbohydrate–functionalized gold, silver, and semiconductor nanoparticles.[204,205] Glyconanoparticles provide a versatile adjustable biomimetic model for the presentation of carbohydrates on cell surfaces and have been used for the investigation of carbohydrate–carbohydrate and carbohydrate–protein interactions.[205–207] They have been used as biomarkers and biosensors, for example, for the detection of concavalin A and *Escherichia coli*[208] as well as in applications in biomedicine and materials science.[205] Dernedde et al. could show by the multivalent presentation of selectins on gold nanoparticles that the IC_{50} values of selectins could be better optimized than with free selectins in the micromolar to picomolar range.[209] A further increase in binding affinity and, above all, a much higher selectivity towards P- rather than L-selectins could also be reached by immobilizing sulfated carbohydrates on gold nanoparticles (Figure 24).[210,211]

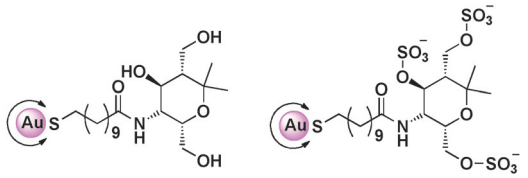

Figure 24. Carbohydrate mimetics, which have been immobilized on gold nanoparticles, with binding affinities in the nano- (left) or picomolar (right) range and with a good P-selectin selectivity.

While the monovalent ligands do not show any binding affinities, there is an IC_{50} value of 10 nM for P-selectin with multivalent ligands bound to gold colloids. The corresponding sulfated system is not only substantially more stable, it also interacts much more strongly to P-selectin ($IC_{50} = 0.04$ nM) and slightly less so with L-selectin ($IC_{50} = 0.35$ nM). Numerous applications in the life sciences require nanoparticles that are permanently stable even under physiological conditions, that is, with relatively high salinity and at temperatures around 37 °C. To meet these requirements, organic ligands, which are necessary for the kinetic stability of the particles, must be firmly bound to the particles. Furthermore, these monovalent bonds are often not sufficient, because there is a chemical equilibrium between particle-bound and free ligands. This balance can be greatly increased in favor of particle-bound molecules by choosing stronger binding multivalent ligands. The particles obtained can thus meet the higher demands. Gubala et al. were able to show that the colloidal stability of nanoparticles could be dramatically increased by using mutivalent dendron ligands instead of monovalent molecules. Furthermore, the detection limit of the assay can be significantly reduced with a more stable, multivalent interaction of the antibodies on the nanoparticle surface, which is required for detection in the immunoassay.[212]

Since nanoparticles can be applied and defined in terms of size and shape, as well as in the chemical composition of their surface, and can be easily detected experimentally by many experimental methods (see Section 2.5), they are an attractive model system for a systematic investigation of multivalent binding effects. Boal and Rotello showed that the multivalent recognition of guest molecules decreased with the radial distance from the particle surface. Thus, they were able to demonstrate that a reduction in the preorganization of the multivalent interaction sites leads to a decrease in the multivalent recognition.[213] Zhang et al. demonstrated in systematic studies on gold particles which had been stabilized by thiol ligands that the colloidal stability is increased by multivalent binding.[67]

Another recent example are gold nanoparticles functionalized with sialic acid (Figure 25 a), which showed a strong interaction with the hemagglutinin surface protein of the influenza virus. Transmission electron microscopy (TEM) was used to visualize the simple attachment with small (ca. 2 nm diameter) gold nanoparticles, whereby the particles could be

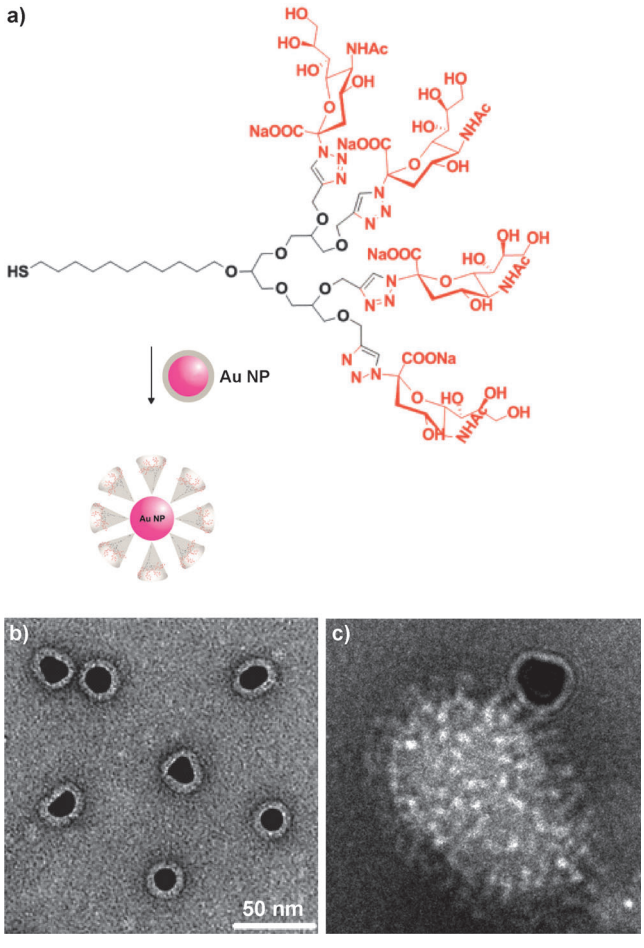

Figure 25. a) Synthesis of sialic acid functionalized gold nanoparticles (AuNPs), b) electron microscopic visualization of 14 nm sized AuNPs, and c) cryo-TEM images of AuNP–virion complexes allow the visualization of single multivalent bonds for the first time.

observed as small black dots on the viral envelope.[80] When large gold colloids were used, however, the single multivalent interactions could be visualized for the first time (Figure 25c). Surprisingly, the 2D image only showed three effective bonds (three to five bonds are spatially possible). This result also shows that spherical multivalent nanoparticles, which are not deformable, are unsuitable for planar interfacial polyvalent interactions, as there are only a few effective interaction points because of the convex surface.

In addition to the particle curvature of "hard-matter" nanoparticles, the limited size of the previously used "soft-matter" polymer particles also limits the reinforcement of the multivalent binding. The distribution of the hemagglutinin receptors on the virus surface does not allow low-valent systems to efficiently interact with multiple trivalent receptors (see Section 4.3). Therefore, large multivalent soft-matter systems would be ideal candidates.

Statistical random polymers (Section 3.1), such as linear polyacrylamide–sialic acid conjugates with high molecular weight (10^6 Da), show a 10^8-fold increase in binding affinity and block cell adhesion through large interfacial, polyvalent interactions. The high molecular weight of the polymer and thus the related long residence time in the body make in vivo applications unrealistic. Nevertheless, the high effectiveness of these linear polymers in vitro has been proven.[86,214] In addition to their extreme affinity binding, they can sterically shield the virus particles when used in combination with other monovalent ligands.[215]

An alternative approach to high-molecular-weight linear polymers are dendritic nanogels that have the same dimensions as influenza viruses and can partake in competitive surface interactions (Figure 26). Novel biocompatible and biodegradable nanogels based on polyglycerol (20 to 100 nm) that can be decorated with the appropriate sialic acid ligand by a simple modular functionalization at their surfaces have been developed in some fundamental studies.[217,218] For the first time, strong interactions could be achieved between the sialic acid functionalized nanogels and the hemagglutinin of influenza virus receptors, and cellular infection could be inhibited up to 80%.[216] It is interesting that nanogels with low functionalization performed better than highly functionalized ones, which may have been due to steric overloading of the latter. These polyvalent nanogels are promising candidates for more effective antiviral therapies.

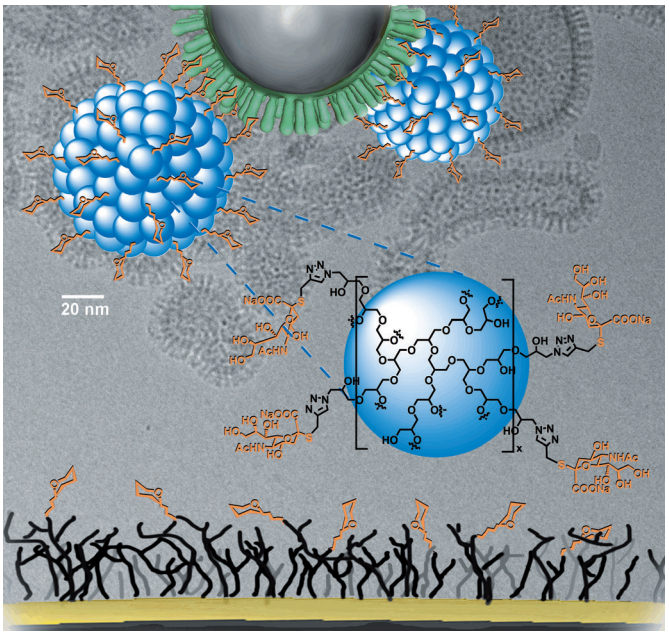

Figure 26. A polyvalent interaction of sialic acid functionalized polyglycerol nanogels with hemagglutinin receptors on the virus surface. The viral binding and thus the cellular infection of the influenza virus can be reduced by up to 80% through efficient competition between the nanogel and glycan structures, such as sLe^x, presented on the cell surface.

4.3. Prospects for Multivalent Drugs

Despite long-standing, fundamental research on multivalent drugs, no major pharmaceutical company has seriously engaged itself yet with the great potential of multivalent interactions. The reason probably lies in the extreme focus that was first on "small molecules" and nowadays on "biologicals." The emerging field of polymer therapeutics has, therefore, been taken up more by innovative small and medium-sized enterprises. Two examples of multivalent drugs will be given.

In analogy to sulfated multivalent glycoconjugates (see Section 4.2, Figure 23), it was possible to synthesize a simple polysulfated heparin analogue stucture.[201] Recently, a highly active anti-inflammatory interaction with dendritic polyglycerol sulfate (dPGS; Figure 27) was discovered which bound other inflammatory mediators in the nanomolar range of L- and P-selectins, as well as in an in vivo mouse model with contact dermatitis that was as effective as the commercial glucocorticoid prednisolone.[72] The great advantages of dPGS are that it is easily obtainable on a large scale and that it is possible to conjugate effector molecules, for example, dyes and drugs.[219]

There has also been a first clinical development of multivalent drugs in the antiviral area. VivaGel was developed as a topical vaginal gel that can prevent or reduce the transmission of HIV. The sulfonated dendritic scaffold is currently being tested in a clinical phase II study.[220] The limited size of the low-generation dendrimers used compared to the distribution of hemagglutinin receptor sites on the virus surface is a limitation for efficient multivalent interactions (Figure 28). However, the elimination of such polymeric drugs through the kidneys is a general consideration that has to be kept in mind (limit is 40 kDa). For future investigations, biodegradable, polyvalent soft-matter systems with large interfacial contact sides should be designed.

5. Conclusion and Outlook

Since the groundbreaking review in 1998 on biologically relevant multivalent systems by Whitesides and co-workers,[1] the multivalency phenomenon has been studied intensively in many new systems. Multivalency has increasingly played

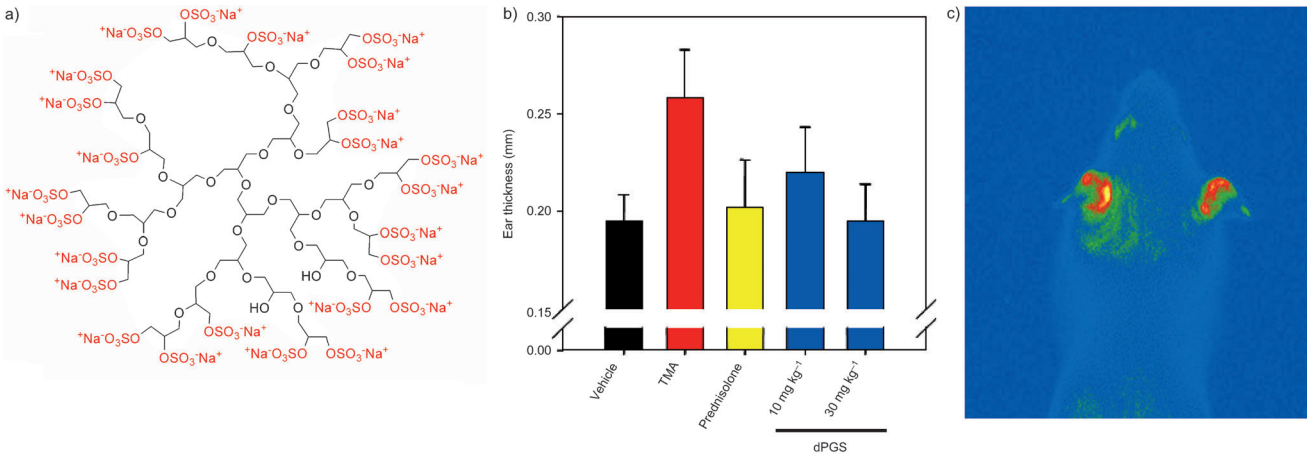

Figure 27. a) Structure of DPGS, b) therapeutic study of contact dermatitis in a mouse model involving ear swelling after stimulation by trimellin acid anhydride (TMA) and dPGS (blue bar) compared to commercial prednisolone (dose: 30 mg kg^{-1}, yellow bar), and c) an inflammation-selective fluorescence diagnosis with a dPGS–dye conjugate.

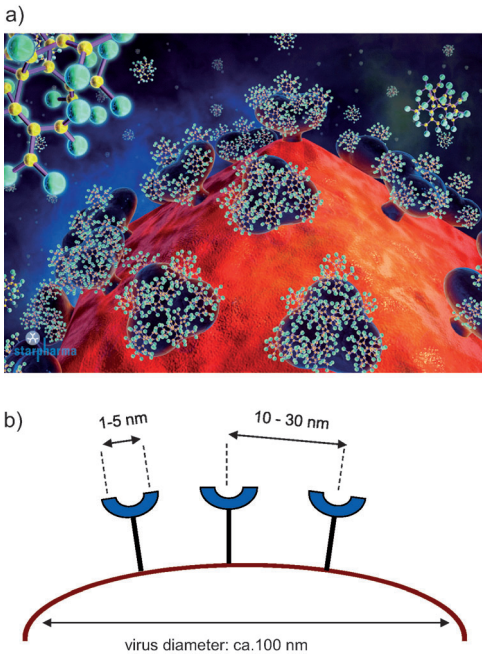

Figure 28. a) The size ratio between the HI virus particle with its trivalent surface receptors and a dendritic drug conjugate (VivaGel, by courtesy of Starpharma) and b) the schematic length ratios for the binding sides within one and between two hemagglutinin receptors on the virus surface.

a major role not only in biological but also in artificial system research areas such as supramolecular chemistry and materials science.

Theoretical studies on the experimental results have begun to generate a deeper understanding of multivalency. There are still only a few reports, however, that make predictions or a reliable plan for the next chemical step. Therefore, systematic studies on models and complex systems are especially necessary for a better knowledge of multivalency, which is paramount for building a theoretical foundation. A joint analysis of the kinetics, thermodynamics, and static effects is also crucial.

Multivalent ligands are clearly more advantageous than monovalent ones because of their enormous binding strength through rigid, defined spacers, and these ligands are increasingly being applied for pharmaceutically relevant targets. Furthermore, the "programmability" of rigid spacers, in other words, the fixed adjustment of the distance between two ligands, makes it now possible to exactly fit the estimated gap between multivalent binding sites, namely, protein complexes. Particularly in heteromultivalent systems, orthogonal binding sites can be built to help maintain the "self-sorting", defined, programmed super lattices.

The exact positioning of multivalent ligands on defined biological scaffolds, such as proteins and DNA, will play an even greater role in the future. Many breakthroughs have occurred in recent years in the area of polyvalent systems with extensive interactions. For example, customized interactions with viral systems have been achieved by the synthesis of tailor-made, multifunctional nano- and microgels. Architectures with a matching size are particularly attractive in this case, as they are also present in biological systems. Interaction is still limited though, because the contact area between spherical particles is relatively small (Figure 25c). Thus, multivalent scaffold architectures with a nonspherical geometry will be especially important in the future.

Biodegradable multivalent nanoparticles are of great significance for use in in vivo polyvalent systems on biological interfaces (such as viruses and bacteria). The excretory organs (kidneys, spleen, liver), however, put strict limits on the particle size.

The first successful clinical studies on multivalent drugs have begun to appear. However, such new drug concepts are only possible if there is a new mindset in the pharmaceutical industry. After a strong focus on "small molecules" and now on "biologicals", polymer therapeutics and multi- and polyvalent drugs in particular have great future potential.

We would like to thank the Deutsche Forschungsgemeinschaft (DFG) for financial support within the Collaborative Research Center 765 and all the participating co-workers for their scientific contributions. We are grateful to Dr. Pamela Winchester for translating this Review.

Received: February 9, 2012
Published online: September 5, 2012

[1] M. Mammen, S.-K. Choi, G. M. Whitesides, *Angew. Chem.* **1998**, *110*, 2908 – 2953; *Angew. Chem. Int. Ed.* **1998**, *37*, 2754 – 2794.
[2] A. Joshi, D. Vance, P. Rai, A. Thiyagarajan, R. S. Kane, *Chem. Eur. J.* **2008**, *14*, 7738 – 7747.
[3] L. L. Kiessling, J. E. Gestwicki, L. E. Strong, *Angew. Chem.* **2006**, *118*, 2408 – 2429; *Angew. Chem. Int. Ed.* **2006**, *45*, 2348 – 2368.
[4] H.-J. Schneider, *Angew. Chem.* **2009**, *121*, 3982 – 4036; *Angew. Chem. Int. Ed.* **2009**, *48*, 3924 – 3977.
[5] J. D. Badjić, A. Nelson, S. J. Cantrill, W. B. Turnbull, J. F. Stoddart, *Acc. Chem. Res.* **2005**, *38*, 723 – 732.
[6] A. Mulder, J. Huskens, D. N. Reinhoudt, *Org. Biomol. Chem.* **2004**, *2*, 3409 – 3424.
[7] J. Huskens, *Curr. Opin. Chem. Biol.* **2006**, *10*, 537 – 543.
[8] N. Jayaraman, *Chem. Soc. Rev.* **2009**, *38*, 3463 – 3483.
[9] a) P. I. B. Kitov, D. R. Bundle *Carbohydrate-Based Drug Discovery* (Ed.: C.-H. Wong), Wiley-VCH, Weinheim, **2005**, pp. 541 – 574; b) V. M. E. Krishnamurthy, L. A. Estroff, G. M. Whitesides, *Fragment-based Approaches in Drug Discovery, 1st ed.* (Eds.: W. E. Jahnke, D. A. Erlanson), Wiley-VCH, Weinheim, **2006**, pp. 11 – 53.
[10] S.-K. Choi, *Synthetic Multivalent Molecules, 1st ed.*, John Wiley & Sons, Hoboken, New Jersey, **2004**..
[11] G. Ercolani, C. Piguet, M. Borkovec, J. Hamacek, *J. Phys. Chem. B* **2007**, *111*, 12195 – 12203.
[12] G. Ercolani, *J. Am. Chem. Soc.* **2003**, *125*, 16097 – 16103.
[13] S. W. Benson, *J. Am. Chem. Soc.* **1958**, *80*, 5151 – 5154.
[14] G. Schwarzenbach, *Anal. Chim. Acta* **1952**, *7*, 141 – 155.
[15] J. Hall, P. A. Karplus, E. Barbar, *J. Biol. Chem.* **2009**, *284*, 33115 – 33121.
[16] T. Christensen, D. M. Gooden, J. E. Kung, E. J. Toone, *J. Am. Chem. Soc.* **2003**, *125*, 7357 – 7366.
[17] V. Vallet, U. Wahlgren, I. Grenthe, *J. Am. Chem. Soc.* **2003**, *125*, 14941 – 14950.
[18] For an detailed analysis of the positively cooperating examples described here, see Ref. [12]. The classic scenario for the cooperativity of a ligand binding does not require multivalency. In fact, it already exists when a multivalent receptor interacts with monomer ligands, whereby the number of already bound ligands increases the strength of the binding accordingly. A prime example for such a behavior is tetravelent hemoglobin. An *n*-valent binding is generally stronger than the corresponding monovalent binding. It will never be so strong, however, that the *n*-fold of monovalent binding energy is reached. Positive cooperativity only first occurs in a multivalent binding if the *n*-valent binding is greater than the *n*-fold of the monovalent binding. Contrary to the norm, multivalent bindings show negative cooperativity (see Ref. [36]). This does not diminish the huge advantage gained from the binding strength of two multivalent objects.
[19] D. J. Diestler, E. W. Knapp, *Phys. Rev. Lett.* **2008**, *100*, 178101.
[20] G. Schwarzenbach, *Helv. Chim. Acta* **1952**, *35*, 2344 – 2363.
[21] O. Andersen, *Chem. Rev.* **1999**, *99*, 2683 – 2710.
[22] J. D. Dunitz, *Chem. Biol.* **1995**, *2*, 709 – 712.
[23] W. E. Stites, *Chem. Rev.* **1997**, *97*, 1233 – 1250.
[24] R. H. Kramer, J. W. Karpen, *Nature* **1998**, *395*, 710 – 713.
[25] W. Kuhn, *Kolloid-Z.* **1934**, *68*, 2 – 15.
[26] M. A. Winnik, *Chem. Rev.* **1981**, *81*, 491 – 524.
[27] J. M. Gargano, T. Ngo, J. Y. Kim, D. W. Acheson, W. J. Lees, *J. Am. Chem. Soc.* **2001**, *123*, 12909 – 12910.
[28] E. T. Mack, P. W. Snyder, R. Perez-Castillejos, G. M. Whitesides, *J. Am. Chem. Soc.* **2011**, *133*, 11701 – 11715.
[29] S. Knecht, D. Ricklin, A. N. Eberle, B. Ernst, *J. Mol. Recognit.* **2009**, *22*, 270 – 279.
[30] F. Noe, C. Schütte, E. Vanden-Eijnden, L. Reich, T. R. Weikl, *Proc. Natl. Acad. Sci. USA* **2009**, *106*, 19011 – 19016.
[31] J. D. Chodera, W. C. Swope, J. W. Pitera, K. A. Dill, *Multiscale Model. Simul.* **2006**, *5*, 1214 – 1226.
[32] W. C. Swope, J. W. Pitera, F. Suits, *J. Phys. Chem. B* **2004**, *108*, 6571 – 6581.
[33] E. Vanden-Eijnden, M. Venturoli, *J. Chem. Phys.* **2009**, *130*, 194101.
[34] M. Weber, S. Kube, *Int. Conf. on Num. Analy. and Appl. Math., Vol. 1048* (Ed.: T. E. Simos; G. Psihoyios; C. Tsitouras), AIP Conference Proceedings, American Institute of Physics, New York, **2008**, pp. 593 – 596.
[35] M. Weber, Habilitation, Freie Universität Berlin, **2011**.
[36] C. A. Hunter, H. L. Anderson, *Angew. Chem.* **2009**, *121*, 7624 – 7636; *Angew. Chem. Int. Ed.* **2009**, *48*, 7488 – 7499.
[37] G. Ercolani, L. Schiaffino, *Angew. Chem.* **2011**, *123*, 1800 – 1807; *Angew. Chem. Int. Ed.* **2011**, *50*, 1762 – 1768.
[38] K. N. W. Jiang, N. L. Löw, E. V. Dzyuba, F. Klautzsch, A. Schäfer, J. Huuskonen, K. Rissanen, C. A. Schalley, *J. Am. Chem. Soc.* **2012**, *134*, 1860 – 1868.
[39] E. Chekmeneva, C. A. Hunter, M. J. Packer, S. M. Turega, *J. Am. Chem. Soc.* **2008**, *130*, 17718 – 17725.
[40] C. A. Hunter, M. C. Misuraca, S. M. Turega, *J. Am. Chem. Soc.* **2011**, *133*, 582 – 594..
[41] M. C. Misuraca, T. Grecu, Z. Freixa, V. Garavini, C. A. Hunter, P. W. van Leeuwen, M. D. Segarra-Maset, S. M. Turega, *J. Org. Chem.* **2011**, *76*, 2723 – 2732.
[42] H. J. Hogben, J. K. Sprafke, M. Hoffmann, M. Pawlicki, H. L. Anderson, *J. Am. Chem. Soc.* **2011**, *133*, 20962 – 20969.
[43] J. K. Sprafke, B. Odell, T. D. Claridge, H. L. Anderson, *Angew. Chem.* **2011**, *123*, 5687 – 5690; *Angew. Chem. Int. Ed.* **2011**, *50*, 5572 – 5575.
[44] C. A. Hunter, M. C. Misuraca, S. M. Turega, *J. Am. Chem. Soc.* **2011**, *133*, 582 – 594.
[45] C. A. Hunter, M. C. Misureca, S. M. Turega, *Chem. Sci.* **2012**, *3*, 589 – 601.
[46] P. J. Flory, *Proc. R. Soc. London Ser. A* **1956**, *234*, 60 – 73.
[47] G. J. Fleer, *Colloid Surf.* **1989**, *35*, 151 – 167.
[48] C. D. Eads, *J. Phys. Chem. B* **2000**, *104*, 6653 – 6661.
[49] D. G. Covell, R. L. Jernigan, *Biochemistry* **1990**, *29*, 3287 – 3294.
[50] D. S. Rykunov, B. A. Reva, A. V. Finkelstein, *Proteins Struct. Funct. Bioinf.* **1995**, *22*, 100 – 109.
[51] T. Schlick, *Molecular Modeling and Simulation: An Interdisciplinary Guide, Vol. 21, 2nd ed.*, Springer, Berlin, **2002**.
[52] W. Göpel, H.-D. Wiemhöfer, *Statistische Thermodynamik*, Spektrum Akademischer Verlag, Heidelberg, **2000**.
[53] M. E. Tuckerman, *Statistical Mechanics: Theory and Molecular Simulation*, Oxford University Press, Oxford, **2010**.
[54] W. Fischer, M. Calderon, A. Schulz, I. Andreou, M. Weber, R. Haag, *Bioconjugate Chem.* **2010**, *21*, 1744 – 1752.
[55] A. Bujotzek, M. Shan, R. Haag, M. Weber, *J. Comput.-Aided Mol. Des.* **2011**, *25*, 253 – 262.
[56] C. Chipot, A. Pohorille, *Free Energy Calculations: Theory and Applications in Chemistry and Biology*, Springer, Berlin, **2007**.
[57] W. H. C. Schütte in *Handbook of Numerical Analysis, Special Volume Computational Chemistry, Vol. 10* (Ed.: P. G. Ciarlet), Elsevier Science & Technology, Amsterdam, **2003**, p. 1032.

[58] P. S. Deuflhard in *Applied Mathematics Entering the 21st Century, Invited Talks from the ICIAM 2003 Congress, Vol. 116* (Eds.: R. Moore, J. M. Hill), Proceedings in Applied Mathematics, Society for Industrial and Applied Mathematics, Philadelphia, **2004**, pp. 91 – 120.
[59] A. W. Bujotzek, M. Weber, *J. Bioinf. . Comput. Biol.* **2009**, *7*, 811 – 831.
[60] A. Robinson, J. M. Fang, P. T. Chou, K. W. Liao, R. M. Chu, S. J. Lee, *ChemBioChem* **2005**, *6*, 1899 – 1905.
[61] M. Gavutis, S. Lata, J. Piehler, *Nat. Protoc.* **2006**, *1*, 2091 – 2103.
[62] H. Jung, A. D. Robison, P. S. Cremer, *J. Struct. Biol.* **2009**, *168*, 90 – 94.
[63] L. Yu, M. Huang, P. G. Wang, X. Zeng, *Anal. Chem.* **2007**, *79*, 8979 – 8986.
[64] N. J. de Mol, F. J. Dekker, I. Broutin, M. J. E. Fischer, R. M. J. Liskamp, *J. Med. Chem.* **2005**, *48*, 753 – 763.
[65] F. P. Schmidtchen in *Analytical Methods in Supramolecular Chemistry* (Ed.: C. A. Schalley), Wiley-VCH, Weinheim, **2007**, pp. 55 – 78.
[66] H. Handa, S. Gurczynski, M. P. Jackson, G. Z. Mao, *Langmuir* **2010**, *26*, 12095 – 12103.
[67] S. S. Zhang, G. Leem, L. O. Srisombat, T. R. Lee, *J. Am. Chem. Soc.* **2008**, *130*, 113 – 120.
[68] C. Scheibe, A. Bujotzek, J. Dernedde, M. Weber, O. Seitz, *Chem. Sci.* **2011**, *2*, 770 – 775.
[69] P. G. A. Janssen, N. J. M. Brankaert, X. Vila, A. Schenning, *Soft Matter* **2010**, *6*, 1494 – 1502.
[70] M. Pittelkow, C. B. Nielsen, A. C. Broeren, J. L. J. van Dongen, M. H. P. van Genderen, E. W. Meijer, J. B. Christensen, *Chem. Eur. J.* **2005**, *11*, 5126 – 5135.
[71] O. Nahshol, V. Bronner, A. Notcovich, L. Rubrecht, D. Laune, T. Bravman, *Anal. Biochem.* **2008**, *383*, 52 – 60.
[72] J. Dernedde, A. Rausch, M. Weinhart, S. Enders, R. Tauber, K. Licha, M. Schirner, U. Zugel, A. von Bonin, R. Haag, *Proc. Natl. Acad. Sci. USA* **2010**, *107*, 19679 – 19684.
[73] Y. Cohen, L. Avram, T. Evan-Salem, L. Frish, *Analytical Methods in Supramolecular Chemistry* (Ed.: C. A. Schalley), Wiley-VCH, Weinheim, **2007**, pp. 163 – 219.
[74] K. Hirose in *Analytical Methods in Supramolecular Chemistry* (Ed.: C. A. Schalley), Wiley-VCH, Weinheim, **2007**, pp. 17 – 54.
[75] T. Evan-Salem, I. Baruch, L. Avram, Y. Cohen, L. C. Palmer, J. Rebek, *Proc. Natl. Acad. Sci. USA* **2006**, *103*, 12296 – 12300.
[76] P. Braun, B. Nägele, V. Wittmann, M. Drescher, *Angew. Chem.* **2011**, *123*, 8579 – 8582; *Angew. Chem. Int. Ed.* **2011**, *50*, 8428 – 8431.
[77] J. Voskuhl, M. C. A. Stuart, B. J. Ravoo, *Chem. Eur. J.* **2010**, *16*, 2790 – 2796.
[78] W. Jiang, K. Nowosinski, N. L. Löw, E. V. Dzyuba, F. Klautzsch, A. Schäfer, J. Huuskonen, K. Rissanen, C. A. Schalley, *J. Am. Chem. Soc.* **2012**, *134*, 1860 – 1868.
[79] Y. H. Zhang, Y. Yu, Z. H. Jiang, H. P. Xu, Z. Q. Wang, X. Zhang, M. Oda, T. Ishizuka, D. L. Jiang, L. F. Chi, H. Fuchs, *Langmuir* **2009**, *25*, 6627 – 6632.
[80] I. Papp, C. Sieben, K. Ludwig, M. Roskamp, C. Böttcher, S. Schlecht, A. Herrmann, R. Haag, *Small* **2010**, *6*, 2900 – 2906.
[81] K. Niikura, K. Nagakawa, N. Ohtake, T. Suzuki, Y. Matsuo, H. Sawa, K. Ijiro, *Bioconjugate Chem.* **2009**, *20*, 1848 – 1852.
[82] H. A. Gussin, I. D. Tomlinson, N. J. Muni, D. M. Little, H. H. Qian, S. J. Rosenthal, D. R. Pepperberg, *Bioconjugate Chem.* **2010**, *21*, 1455 – 1464.
[83] J. J. Shi, T. L. Yang, S. Kataoka, Y. J. Zhang, A. J. Diaz, P. S. Cremer, *J. Am. Chem. Soc.* **2007**, *129*, 5954 – 5961.
[84] J. Rao, J. Lahiri, L. Isaacs, R. M. Weis, G. M. Whitesides, *Science* **1998**, *280*, 708 – 711.
[85] G. B. Sigal, M. Mammen, G. Dahmann, G. M. Whitesides, *J. Am. Chem. Soc.* **1996**, *118*, 3789 – 3800.
[86] S. K. Choi, M. Mammen, G. M. Whitesides, *J. Am. Chem. Soc.* **1997**, *119*, 4103 – 4111.
[87] See Ref. [3].
[88] K. Wu, J. Liu, R. N. Johnson, J. Yang, J. Kopeček, *Angew. Chem.* **2010**, *122*, 1493 – 1497; *Angew. Chem. Int. Ed.* **2010**, *49*, 1451 – 1455.
[89] R. Narain, *Engineered carbohydrate-based materials for biomedical applications*: *polymers, surfaces, dendrimers, nanoparticles, and hydrogels*, Wiley, Hoboken, **2011**.
[90] L. Röglin, E. H. M. Lempens, E. W. Meijer, *Angew. Chem.* **2011**, *123*, 106 – 117; *Angew. Chem. Int. Ed.* **2011**, *50*, 102 – 112.
[91] *Glycoscience and Microbial Adhesion*, *Vol. 288*, (Eds.: T. K. Lindhorst, S. Oscarson), Springer, Berlin, **2009**.
[92] J. J. Landers, Z. Y. Cao, I. Lee, L. T. Piehler, P. P. Myc, A. Myc, T. Hamouda, A. T. Galecki, J. R. Baker, *J. Infect. Dis.* **2002**, *186*, 1222 – 1230.
[93] M. Cloninger, *Drug Discovery Today* **2004**, *9*, 111 – 112.
[94] Z. Poon, S. Chen, A. C. Engler, H. I. Lee, E. Atas, G. von Maltzahn, S. N. Bhatia, P. T. Hammond, *Angew. Chem.* **2010**, *122*, 7424 – 7428; *Angew. Chem. Int. Ed.* **2010**, *49*, 7266 – 7270.
[95] D. Zacher, R. Schmid, C. Woll, R. A. Fischer, *Angew. Chem.* **2011**, *123*, 184 – 208; *Angew. Chem. Int. Ed.* **2011**, *50*, 176 – 199.
[96] L. Vandromme, H. U. Reißig, S. Groper, J. P. Rabe, *Eur. J. Org. Chem.* **2008**, 2049 – 2055.
[97] X. C. Zhou, C. Turchi, D. N. Wang, *J. Proteome Res.* **2009**, *8*, 5031 – 5040.
[98] M. H. Park, X. X. Duan, Y. Ofir, B. Creran, D. Patra, X. Y. Ling, J. Huskens, V. M. Rotello, *ACS Appl. Mater. Interfaces* **2010**, *2*, 795 – 799.
[99] D. Dorokhin, S. H. Hsu, N. Tomczak, D. N. Reinhoudt, J. Huskens, A. H. Velders, G. J. Vancso, *ACS Nano* **2010**, *4*, 137 – 142.
[100] T. A. Klar, T. Franzl, A. L. Rogach, J. Feldmann, *J. Adv. Mater.* **2005**, *17*, 769 – 773.
[101] X. Wang, C. J. Summers, Z. L. Wang, *Nano Lett.* **2004**, *4*, 423 – 426.
[102] E. Russ Galian, M. de La Guardia, *TrAC Trends Anal. Chem.* **2009**, *28*, 279 – 291.
[103] W. R. Algar, M. Massey, U. J. Krull, *TrAC Trends Anal. Chem.* **2009**, *28*, 292 – 306.
[104] P. A. Johnson, R. Levicky, *Langmuir* **2003**, *19*, 10288 – 10294.
[105] S. C. Wagner, M. Roskamp, H. Colfen, C. Bottcher, S. Schlecht, B. Koksch, *Org. Biomol. Chem.* **2009**, *7*, 46 – 51.
[106] R. T. Lee, Y. C. Lee, *Methods Enzymol.* **2003**, *362*, 38 – 43.
[107] J. J. Hangeland, J. E. Flesher, S. F. Deamond, Y. C. Lee, O. P. Ts, J. J. Frost, *Antisense Nucleic Acid Drug Dev.* **1997**, *7*, 141 – 149.
[108] J. P. Tam, *Proc. Natl. Acad. Sci. USA* **1988**, *85*, 5409 – 5413.
[109] G. Thumshirn, U. Hersel, S. L. Goodman, H. Kessler, *Chem. Eur. J.* **2003**, *9*, 2717 – 2725.
[110] P. Niederhafner, J. Šebestík, J. Ježek, *J. Pept. Sci.* **2008**, *14*, 2 – 43.
[111] P. Niederhafner, J. Šebestík, J. Ježek, *J. Pept. Sci.* **2008**, *14*, 44 – 65.
[112] H. Kamitakahara, T. Suzuki, N. Nishigori, Y. Suzuki, O. Kanie, C.-H. Wong, *Angew. Chem.* **1998**, *110*, 1607 – 1611; *Angew. Chem. Int. Ed.* **1998**, *37*, 1524 – 1528.
[113] K. Totani, T. Kubota, T. Kuroda, T. Murata, K. I. Hidari, T. Suzuki, Y. Suzuki, K. Kobayashi, H. Ashida, K. Yamamoto, T. Usui, *Glycobiology* **2003**, *13*, 315 – 326.
[114] B. D. Polizzotti, K. L. Kiick, *Biomacromolecules* **2006**, *7*, 483 – 490.
[115] X. Zeng, Y. Nakaaki, T. Murata, T. Usui, *Arch. Biochem. Biophys.* **2000**, *383*, 28 – 37.
[116] X. Zeng, T. Murata, H. Kawagishi, T. Usui, K. Kobayashi, *Carbohydr. Res.* **1998**, *312*, 209 – 217.
[117] a) N. Voyer, J. Lamothe, *Tetrahedron* **1995**, *51*, 9241 – 9284; b) N. Voyer, *Top. Curr. Chem.* **1996**, *184*, 1 – 37.

[118] C. Unverzagt, S. Kelm, J. C. Paulson, *Carbohydr. Res.* **1994**, *251*, 285 – 301.
[119] S. Liu, K. L. Kiick, *Macromolecules* **2008**, *41*, 764 – 772.
[120] J. A. Falenski, U. I. M. Gerling, B. Koksch, *Bioorg. Med. Chem.* **2010**, *18*, 3703 – 3706.
[121] L. M. Artner, L. Merkel, N. Bohlke, F. Beceren-Braun, C. Weise, J. Dernedde, N. Budisa, C. P. R. Hackenberger, *Chem. Commun.* **2012**, *48*, 522 – 524.
[122] N. C. Seeman, *Nano Lett.* **2010**, *10*, 1971 – 1978.
[123] N. C. Seeman, *Annu. Rev. Biochem.* **2010**, *79*, 65 – 87.
[124] V. L. Malinovskii, D. Wenger, R. Haner, *Chem. Soc. Rev.* **2010**, *39*, 410 – 422.
[125] G. H. Clever, T. Carell, *Angew. Chem.* **2007**, *119*, 254 – 257; *Angew. Chem. Int. Ed.* **2007**, *46*, 250 – 253.
[126] G. H. Clever, C. Kaul, T. Carell, *Angew. Chem.* **2007**, *119*, 6340 – 6350; *Angew. Chem. Int. Ed.* **2007**, *46*, 6226 – 6236.
[127] C. M. Niemeyer, *Angew. Chem.* **2010**, *122*, 1220 – 1238; *Angew. Chem. Int. Ed.* **2010**, *49*, 1200 – 1216.
[128] L. Röglin, O. Seitz, *Org. Biomol. Chem.* **2008**, *6*, 3881 – 3887.
[129] F. Diezmann, O. Seitz, *Chem. Soc. Rev.* **2011**, *40*, 5789 – 5801.
[130] H. G. Hansma, K. J. Kim, D. E. Laney, R. A. Garcia, M. Argaman, M. J. Allen, S. M. Parsons, *J. Struct. Biol.* **1997**, *119*, 99 – 108.
[131] Y. J. Lu, B. Weers, N. C. Stellwagen, *Biopolymers* **2001**, *61*, 261 – 275.
[132] T. Akasaka, K. Matsuura, K. Kobayashi, *Bioconjugate Chem.* **2001**, *12*, 776 – 785.
[133] K. Matsuura, M. Hibino, Y. Yamada, K. Kobayashi, *J. Am. Chem. Soc.* **2001**, *123*, 357 – 358.
[134] K. Matsuura, M. Hibino, T. Ikeda, Y. Yamada, K. Kobayashi, *Chem. Eur. J.* **2004**, *10*, 352 – 359.
[135] Y. Yamada, K. Matsuura, K. Kobayashi, *Bioorg. Med. Chem.* **2005**, *13*, 1913 – 1922.
[136] K. Gorska, K. T. Huang, O. Chaloin, N. Winssinger, *Angew. Chem.* **2009**, *121*, 7831 – 7836; *Angew. Chem. Int. Ed.* **2009**, *48*, 7695 – 7700.
[137] K. Gorska, J. Beyrath, S. Fournel, G. Guichard, N. Winssinger, *Chem. Commun.* **2010**, *46*, 7742 – 7744.
[138] E. A. Englund, D. Wang, H. Fujigaki, H. Sakai, C. M. Micklitsch, R. Ghirlando, G. Martin-Manso, M. L. Pendrak, D. D. Roberts, S. R. Durell, D. H. Appella, *Nat. Commun.* **2012**, *3*, 614.
[139] H. Eberhard, F. Diezmann, O. Seitz, *Angew. Chem.* **2011**, *123*, 4232 – 4236; *Angew. Chem. Int. Ed.* **2011**, *50*, 4146 – 4150.
[140] F. Abendroth, A. Bujotzek, M. Shan, R. Haag, M. Weber, O. Seitz, *Angew. Chem.* **2011**, *123*, 8751 – 8755; *Angew. Chem. Int. Ed.* **2011**, *50*, 8592 – 8596.
[141] S. Melkko, Y. Zhang, C. E. Dumelin, J. Scheuermann, D. Neri, *Angew. Chem.* **2007**, *119*, 4755 – 4758; *Angew. Chem. Int. Ed.* **2007**, *46*, 4671 – 4674.
[142] L. Mannocci, S. Melkko, F. Buller, I. Molnar, J. P. G. Bianke, C. E. Dumelin, J. Scheuermann, D. Neri, *Bioconjugate Chem.* **2010**, *21*, 1836 – 1841.
[143] K. I. Sprinz, D. M. Tagore, A. D. Hamilton, *Bioorg. Med. Chem. Lett.* **2005**, *15*, 3908 – 3911.
[144] D. M. Tagore, K. I. Sprinz, S. Fletcher, J. Jayawickramarajah, A. D. Hamilton, *Angew. Chem.* **2007**, *119*, 227 – 229; *Angew. Chem. Int. Ed.* **2007**, *46*, 223 – 225.
[145] D. M. Tagore, K. I. Sprinz, A. D. Hamilton, *Supramol. Chem.* **2007**, *19*, 129 – 136.
[146] D. C. Harris, X. Z. Chu, J. Jayawickramarajah, *J. Am. Chem. Soc.* **2008**, *130*, 14950 – 14951.
[147] J. P. Daguer, M. Ciobanu, S. Alvarez, S. Barluenga, N. Winssinger, *Chem. Sci.* **2011**, *2*, 625 – 632.
[148] B. A. R. Williams, C. W. Diehnelt, P. Belcher, M. Greving, N. W. Woodbury, S. A. Johnston, J. C. Chaput, *J. Am. Chem. Soc.* **2009**, *131*, 17233 – 17241.
[149] M. Shan, A. Bujotzek, F. Abendroth, A. Wellner, R. Gust, O. Seitz, M. Weber, R. Haag, *ChemBioChem* **2011**, *12*, 2587 – 2598.
[150] See Ref. [140].
[151] D. Schwefel, C. Maierhofer, J. G. Beck, S. Seeberger, K. Diederichs, H. M. Moller, W. Welte, V. Wittmann, *J. Am. Chem. Soc.* **2010**, *132*, 8704 – 8719.
[152] G. Ercolani, *J. Phys. Chem. B* **2003**, *107*, 5052 – 5057.
[153] J. Huskens, A. Mulder, T. Auletta, C. A. Nijhuis, M. J. W. Ludden, D. N. Reinhoudt, *J. Am. Chem. Soc.* **2004**, *126*, 6784 – 6797.
[154] G. Ercolani, M. Ioele, D. Monti, *New J. Chem.* **2001**, *25*, 783 – 789.
[155] M. Mammen, E. I. Shakhnovich, J. M. Deutch, G. M. Whitesides, *J. Org. Chem.* **1998**, *63*, 3821 – 3830.
[156] A. G. Bielejewska, C. E. Marjo, L. J. Prins, P. Timmerman, F. de Jong, D. N. Reinhoudt, *J. Am. Chem. Soc.* **2001**, *123*, 7518 – 7533.
[157] A. Pfeil, J. M. Lehn, *J. Chem. Soc. Chem. Commun.* **1992**, 838 – 840.
[158] T. M. Garrett, U. Koert, J. M. Lehn, *J. Phys. Org. Chem.* **1992**, *5*, 529 – 532.
[159] N. Fatin-Rouge, S. Blanc, A. Pfeil, A. Rigault, A. M. Albrecht-Gary, J. M. Lehn, *Helv. Chim. Acta* **2001**, *84*, 1694 – 1711.
[160] A. Marquis, J. P. Kintzinger, R. Graff, P. N. W. Baxter, J. M. Lehn, *Angew. Chem.* **2002**, *114*, 2884 – 2888; *Angew. Chem. Int. Ed.* **2002**, *41*, 2760 – 2764.
[161] P. N. Taylor, H. L. Anderson, *J. Am. Chem. Soc.* **1999**, *121*, 11538 – 11545.
[162] A. P. Bisson, F. J. Carver, C. A. Hunter, J. P. Waltho, *J. Am. Chem. Soc.* **1994**, *116*, 10292 – 10293.
[163] A. P. Bisson, C. A. Hunter, J. C. Morales, K. Young, *Chem. Eur. J.* **1998**, *4*, 845 – 851.
[164] M. I. Page, W. P. Jencks, *Proc. Natl. Acad. Sci. USA* **1971**, *68*, 1678 – 1683.
[165] M. S. Searle, D. H. Williams, *J. Am. Chem. Soc.* **1992**, *114*, 10690 – 10697.
[166] F. Eblinger, H. J. Schneider, *Angew. Chem.* **1998**, *110*, 821 – 824; *Angew. Chem. Int. Ed.* **1998**, *37*, 826 – 829.
[167] M. A. Hossain, H. J. Schneider, *Chem. Eur. J.* **1999**, *5*, 1284 – 1290.
[168] J. J. Reczek, A. A. Kennedy, B. T. Halbert, A. R. Urbach, *J. Am. Chem. Soc.* **2009**, *131*, 2408 – 2415.
[169] P. B. Armentrout, *Int. J. Mass Spectrom.* **1999**, *193*, 227 – 240.
[170] C. A. Schalley, A. Springer, *Mass-Spectrometry and Gas-Phase Chemistry of Non-Covalent Complexes*, Wiley, Hoboken, **2009**, pp. 329 – 356.
[171] V. Balzani, M. Clemente-Leon, A. Credi, J. N. Lowe, J. D. Badjic, J. F. Stoddart, D. J. Williams, *Chem. Eur. J.* **2003**, *9*, 5348 – 5360.
[172] J. D. Badjić, V. Balzani, A. Credi, J. N. Lowe, S. Silvi, J. F. Stoddart, *Chem. Eur. J.* **2004**, *10*, 1926 – 1935.
[173] J. D. Badjić, V. Balzani, A. Credi, S. Silvi, J. F. Stoddart, *Science* **2004**, *303*, 1845 – 1849.
[174] J. D. Badjić, C. M. Ronconi, J. F. Stoddart, V. Balzani, S. Silvi, A. Credi, *J. Am. Chem. Soc.* **2006**, *128*, 1489 – 1499.
[175] J. D. Badjić, S. J. Cantrill, J. F. Stoddart, *J. Am. Chem. Soc.* **2004**, *126*, 2288 – 2289.
[176] A. Perl, A. Gomez-Casado, D. Thompson, H. H. Dam, P. Jonkheijm, D. N. Reinhoudt, J. Huskens, *Nat. Chem.* **2011**, *3*, 317 – 322.
[177] A. Gomez-Casado, H. H. Dam, M. D. Yilmaz, D. Florea, P. Jonkheijm, J. Huskens, *J. Am. Chem. Soc.* **2011**, *133*, 10849 – 10857.
[178] X. Y. Ling, D. N. Reinhoudt, J. Huskens, *Pure Appl. Chem.* **2009**, *81*, 2225 – 2233.
[179] S. Kinge, M. Crego-Calama, D. N. Reinhoudt, *ChemPhysChem* **2008**, *9*, 20 – 42.

[180] See Ref. [7].
[181] H. M. Saavedra, T. J. Mullen, P. P. Zhang, D. C. Dewey, S. A. Claridge, P. S. Weiss, *Rep. Prog. Phys.* **2010**, *73*, 036501.
[182] O. Crespo-Biel, B. J. Ravoo, D. N. Reinhoudt, J. Huskens, *J. Mater. Chem.* **2006**, *16*, 3997 – 4021.
[183] O. Crespo-Biel, B. Dordi, D. N. Reinhoudt, J. Huskens, *J. Am. Chem. Soc.* **2005**, *127*, 7594 – 7600.
[184] O. Crespo-Biel, C. W. Lim, B. J. Ravoo, D. N. Reinhoudt, J. Huskens, *J. Am. Chem. Soc.* **2006**, *128*, 17024 – 17032.
[185] a) Y. C. Lee, R. T. Lee, *Acc. Chem. Res.* **1995**, *28*, 321 – 327; b) J. J. Lundquist, E. J. Toone, *Chem. Rev.* **2002**, *102*, 555 – 578.
[186] S. R. S. Ting, G. Chen, M. H. Stenzel, *Polym. Chem.* **2010**, *1*, 1392 – 1412.
[187] a) T. K. Dam, C. F. Brewer, *Advances in Carbohydrate Chemistry and Biochemistry*, *Vol. 63* (Ed.: D. Horton), Academic Press, New York, **2010**, pp. 139 – 164; b) Y. M. Chabre, R. Roy, *Advances in Carbohydrate Chemistry and Biochemistry*, *Vol. 63* (Ed.: D. Horton), Academic Press, New York, **2010**, pp. 165 – 393.
[188] E. A. Merritt, S. Sarfaty, F. van den Akker, C. L'Hoir, J. A. Martial, W. G. Hol, *Protein Sci.* **1994**, *3*, 166 – 175.
[189] P. I. Kitov, J. M. Sadowska, G. Mulvey, G. D. Armstrong, H. Ling, N. S. Pannu, R. J. Read, D. R. Bundle, *Nature* **2000**, *403*, 669 – 672.
[190] W. B. Turnbull, B. L. Precious, S. W. Homans, *J. Am. Chem. Soc.* **2004**, *126*, 1047 – 1054.
[191] A. V. Pukin, H. M. Branderhorst, C. Sisu, C. A. Weijers, M. Gilbert, R. M. Liskamp, G. M. Visser, H. Zuilhof, R. J. Pieters, *ChemBioChem* **2007**, *8*, 1500 – 1503.
[192] C. Sisu, A. J. Baron, H. M. Branderhorst, S. D. Connell, C. A. Weijers, R. de Vries, E. D. Hayes, A. V. Pukin, M. Gilbert, R. J. Pieters, H. Zuilhof, G. M. Visser, W. B. Turnbull, *ChemBioChem* **2009**, *10*, 329 – 337.
[193] H. M. Branderhorst, R. M. Liskamp, G. M. Visser, R. J. Pieters, *Chem. Commun.* **2007**, 5043 – 5045.
[194] T. Lindhorst in *Topics in Current Chemistry*, *Vol. 218* (Ed.: S. Penadés), Springer, Berlin, **2002**, pp. 201 – 235.
[195] K. Elsner, M. M. K. Boysen, T. K. Lindhorst, *Carbohydr. Res.* **2007**, *342*, 1715 – 1725.
[196] I. Deguise, D. Lagnoux, R. Roy, *New J. Chem.* **2007**, *31*, 1321 – 1331.
[197] E. E. Simanek, G. J. McGarvey, J. A. Jablonowski, C. H. Wong, *Chem. Rev.* **1998**, *98*, 833 – 862.
[198] Y. M. Chabre, R. Roy, *Curr. Top. Med. Chem.* **2008**, *8*, 1237 – 1285.
[199] G. Thoma, R. O. Duthaler, J. L. Magnani, J. T. Patton, *J. Am. Chem. Soc.* **2001**, *123*, 10113 – 10114.
[200] I. Papp, J. Dernedde, S. Enders, R. Haag, *Chem. Commun.* **2008**, 5851 – 5853.
[201] H. Türk, R. Haag, S. Alban, *Bioconjugate Chem.* **2004**, *15*, 162 – 167.
[202] M. Weinhart, D. Groger, S. Enders, S. B. Riese, J. Dernedde, R. K. Kainthan, D. E. Brooks, R. Haag, *Macromol. Biosci.* **2011**, *11*, 1088 – 1098.
[203] A. Hofmann, S. Thierbach, A. Semisch, A. Hartwig, M. Taupitz, E. Rühl, C. Graf, *J. Mater. Chem.* **2010**, *20*, 7842 – 7853.
[204] J. M. de la Fuente, A. G. Barrientos, T. C. Rojas, J. Rojo, J. Canada, A. Fernandez, S. Penades, *Angew. Chem.* **2001**, *113*, 2317 – 2321; *Angew. Chem. Int. Ed.* **2001**, *40*, 2257 – 2261.
[205] J. M. de la Fuente, S. Penades, *Biochim. Biophys. Acta Gen. Subj.* **2006**, *1760*, 636 – 651.
[206] R. Kikkeri, P. Laurino, A. Odedra, P. H. Seeberger, *Angew. Chem.* **2010**, *122*, 2098 – 2101; *Angew. Chem. Int. Ed.* **2010**, *49*, 2054 – 2057.
[207] R. Kikkeri, B. Lepenies, A. Adibekian, P. Laurino, P. H. Seeberger, *J. Am. Chem. Soc.* **2009**, *131*, 2110 – 2112.
[208] C. C. Huang, C. T. Chen, Y. C. Shiang, Z. H. Lin, H. T. Chang, *Anal. Chem.* **2009**, *81*, 875 – 882.
[209] J. Dernedde, S. Enders, H. U. Reißig, M. Roskamp, S. Schlecht, S. Yekta, *Chem. Commun.* **2009**, 932 – 934.
[210] M. Roskamp, S. Enders, F. Pfrengle, S. Yekta, V. Dekaris, J. Dernedde, H. U. Reißig, S. Schlecht, *Org. Biomol. Chem.* **2011**, *9*, 7448 – 7456.
[211] See Ref. [209].
[212] V. Gubala, X. Le Guevel, R. Nooney, D. E. Williams, B. MacCraith, *Talanta* **2010**, *81*, 1833 – 1839.
[213] A. K. Boal, V. M. Rotello, *J. Am. Chem. Soc.* **2002**, *124*, 5019 – 5024.
[214] M. Mammen, G. Dahmann, G. M. Whitesides, *J. Med. Chem.* **1995**, *38*, 4179 – 4190.
[215] S. K. Choi, M. Mammen, G. M. Whitesides, *Chem. Biol.* **1996**, *3*, 97 – 104.
[216] I. Papp, C. Sieben, A. L. Sisson, J. Kostka, C. Bottcher, K. Ludwig, A. Herrmann, R. Haag, *ChemBioChem* **2011**, *12*, 887 – 895.
[217] A. L. Sisson, D. Steinhilber, T. Rossow, P. Welker, K. Licha, R. Haag, *Angew. Chem.* **2009**, *121*, 7676 – 7681; *Angew. Chem. Int. Ed.* **2009**, *48*, 7540 – 7545.
[218] D. Steinhilber, A. L. Sisson, D. Mangoldt, P. Welker, K. Licha, R. Haag, *Adv. Funct. Mater.* **2010**, *20*, 4133 – 4138.
[219] K. Licha, P. Welker, M. Weinhart, N. Wegner, S. Kern, S. Reichert, I. Gemeinhardt, C. Weissbach, B. Ebert, R. Haag, M. Schirner, *Bioconjugate Chem.* **2011**, *22*, 2453 – 2460.
[220] a) Further Information under: http://www.starpharma.com; b) T. D. McCarthy, P. Karellas, S. A. Henderson, M. Giannis, D. F. O'Keefe, G. Heery, J. R. A. Paull, B. R. Matthews, G. Holan, *Mol. Pharm.* **2005**, *2*, 312 – 318; c) R. Rupp, S. L. Rosenthal, L. R. Stanberry, *Int. J. Nanomed.* **2007**, *2*, 561 – 566.
[221] M. Weber, A. Bujotzek, R. Haag, *J. Chem. Phys.* **2012**, *137*, 054111.
[222] B. Imperiali, *Acc. Chem. Res.* **1997**, *30*, 452 – 459.